Plasma Physics Issues in Gas Discharge Laser Development

Alan Garscadden, *Senior Member, IEEE*, Mark J. Kushner, *Fellow, IEEE*, and J. Gary Eden, *Fellow, IEEE*

(Invited Review Paper)

***Abstract*—An account is given of the interplay between partially ionized plasma physics and the development of gas discharge lasers. Gas discharge excitation has provided a wide array of laser devices extending from the soft X-ray region to the far infrared. The scaling of gas discharge lasers in power and energy also covers many orders of magnitude. The particular features of three regimes are discussed: short wavelength lasers (deep UV to soft X-ray); visible and near UV lasers; and infrared molecular gas lasers. The current status (Fall 1990) of these areas is reviewed, and an assessment is made of future research topics that are perceived to be important.**

I. Introduction

ALTHOUGH R. C. Tolman [1] appears to have originated in 1923 the concept of population inversion leading to stimulated emission and amplification, his comments suggest that he considered the situation so improbable as to be of little value. However, at about the same time, R. Ladenburg [2] found it necessary when analyzing experiments on anomalous dispersion to include stimulated emission terms in his analyses of radiation from the positive columns of narrow-bore neon discharges. The early discharge investigations of Ladenburg and of V. A. Fabrikant [3] and their colleagues came close to achieving the necessary conditions for population inversion and laser action. At that time, there was emphasis on understanding the approach to equilibrium at higher discharge currents and almost no research on enhancing the nonequilibrium features.

The threshold condition for a gas laser [4] is

$$\frac{N_u}{g_u} - \frac{N_l}{g_l} = \frac{8\pi}{A_{ul} g_u \lambda^3} \left(\frac{2\pi R T_g}{M} \right)^{\frac{1}{2}} \frac{\alpha}{L} \qquad (1)$$

where N_u, g_u, N_l, and g_l are the populations and statistical weights of the upper and lower laser levels, respectively, A_{ul} is the transition probability, R is the gas constant, T_g is the gas temperature, M is the molecular mass, α is the total loss coefficient, and L is the length of the gain medium. Other things being equal, it is much easier to obtain gain at longer wavelengths, since the threshold energy density of the plasma for infrared lasers is much less than that for short wavelength lasers. Shorter wavelengths also require plasma media of high uniformity to avoid beam spreading by refractive inhomogeneities. Consequently, the short wavelength lasers tend to scale with energy density, while the longer wavelength molecular gas lasers can scale both volumetrically and with energy density to the extent that the enhanced plasma chemistry does not deplete or quench the lasing species. Also, the transition probabilities are generally much higher at shorter wavelengths so that it becomes much more difficult to achieve CW operation unless the lower laser level population is rapidly depleted. Therefore as one moves into the UV regime, pulsed laser technology is generally invoked to meet these constraints. Further complications in developing discharge pumped short wavelength lasers are the plasma instabilities associated with intense pumping rates.

Much of the exploratory work on identifying and developing new lasers occurred in the 1960's and 70's, and now the studies are usually confined to a much more limited range of species and gas mixtures. The emphasis has also changed to improving the reliability and lifetime of the laser.

Given the above constraints, one concludes that the electrical discharge laser is superior to chemical lasers under those conditions where energy density scaling is required. Compared to solid-state lasers, it wins when volumetric scaling or operation at short wavelengths ($\lambda < 200$ nm) is required. Discharge lasers also have the advantages that gases can be self-healing and are much more tolerant than solids of thermal overload.

II. Short-Wavelength Lasers in Discharges and Laser-Produced Plasmas: UV to Soft X-Ray

In their classic review paper in 1976, Waynant and Elton [5] discussed the demanding requirements inherent to the demonstration of new lasers in the spectral region below 200 nm. Written on the eve of the discovery of the ArF, ArCl, and KrCl rare gas–halide lasers, their article summarized the properties of the handful of vacuum ultraviolet (VUV) molecular lasers existing at the time (H_2, HD, D_2, CO, Xe_2, Kr_2, Ar_2), but also described with remarkable accuracy the plasma parameters necessary for the successful operation of atomic oscillators at still shorter wavelengths ($\lambda < 100$ nm). The past 15 years have witnessed not only the development of the rare gas–halide excimer and F_2 lasers, but since the 1985

Manuscript received April 24, 1990; revised September 18, 1991. The research of A. G. was supported by the U.S. Air Force Office of Scientific Research (AFOSR) under Project No. 2301, that of J. G. Eden through AFOSR Grant 89–0038 (H. Schlossberg), and that of M. J. Kushner by the National Science Foundation under Contract Nos. ECS 88–15781 and CBT 88–03170.

A. Garscadden is with the Wright Laboratory, Wright-Patterson AFB, OH 45433.

M. J. Kushner and J. G. Eden are with the Department of Electrical and Computer Engineering, University of Illinois, Urbana, IL 61801.

IEEE Log Number 9104618.

report by Matthews *et al.* [6], a succession of XUV and soft X-ray amplifiers and oscillators based on electronic transitions in multiply charged ions. This section will briefly review recent progress in this area (through Fall 1990) and venture a few predictions as to future directions.

A. Atomic Lasers

Short wavelength ($\lambda < 200$ nm) atomic lasers and amplifiers developed in the past decade have relied exclusively on laser-produced plasmas as the excitation source. In most cases, population inversion is achieved by electron-impact excitation of the upper laser level while, in other instances, incoherent soft X-rays produced by the hot, dense plasma photoionize the species of interest. The success of this tool is perhaps best illustrated by noting that, at the time of this writing, more than 35 ionic transitions in the soft X-ray region alone have lased or produced gain.

MacGowan *et al.* [8] have summarized the majority of the ions that have, to date, exhibited amplification in the XUV or soft X-ray regions. By irradiating thin selenium foils mounted on Formvar substrates with $7 \cdot 10^{13}$ W-cm^{-2} of 0.53 μm (frequency doubled Nd:YAG) photons, Matthews *et al.* [6], [9] at the Lawrence Livermore National Laboratory observed amplification on 3p $\rightarrow$ 3s transitions of the Ne-like ion Se^{24+} (Se XXV) at 20.64 and 20.98 nm. Vaporization of the target at such intensities produces plasmas characterized by electron densities of $3 - 5 \cdot 10^{20}$cm^{-3} and a $\sim$ 1-keV electron temperature. Pumping of the $2p^5{}_{1/2}\ 3p_{1/2}$ ($J = 0$) level of the multiply charged Se ion is expected to occur by electron-impact excitation of the ion's $2p^6$ ground state. Spontaneous emission (on the 3s $\rightarrow$ 2p transition) rapidly deactivates the 3s ($J = 1$) lower laser level population of the ion, allowing gain coefficients of ~ 4.0cm^{-1} to be realized on the 20.6-nm transition. Several other Ne-like ions have exhibited gain at wavelengths ranging from 8.2 to 28.5 nm, and Table I (adapted from [8], [10], and [11]) summarizes the results obtained with nine atomic ions. The Zn, Ga, and As oscillator data were obtained in experiments conducted at the Naval Research Laboratory. The spectral region over which gain has been obtained (at discrete wavelengths) is indicated, as is the measured gain coefficient. Also, the rapid rise in peak laser-pump intensity that is required as the gain wavelength decreases is clear from Table I. This trend is supported by Waynant and Elton's [5] calculations in which, in the 1–100 nm region, the volumetric pumping rate was predicted to increase by four orders of magnitude for each factor of ten decrease in wavelength (i.e., 10^7W-cm^{-3} at 100 nm to 10^{11}W-cm^{-3} at 10 nm). Rosen *et al.*'s calculations [12] underscore this behavior as they show that the pump laser power required to reach saturation of a soft X-ray laser scales with wavelength as λ^{-4}.

Fig. 1 (reprinted from [5]) also illustrates the strong functional dependence of the mean plasma density on λ. The variation of peak laser intensity with laser wavelength (shown in Fig. 2 for several Ne-like systems demonstrated to date) qualitatively reflects the increased demands placed on pump power by moving to shorter wavelengths [8], [13]. If the plasma length along the coordinate orthogonal to the optical axis of the laser is $\sim 100\mu$m, then the pump intensities of Table I and Fig. 2 correspond to instantaneous specific power loadings of $6 \cdot 10^{14}$ to $4 \cdot 10^{16}$W-cm^{-3}, which are several orders of magnitude higher than the estimate from [5] of 10^{11}W-cm^{-3} for $\lambda = 10$ nm.

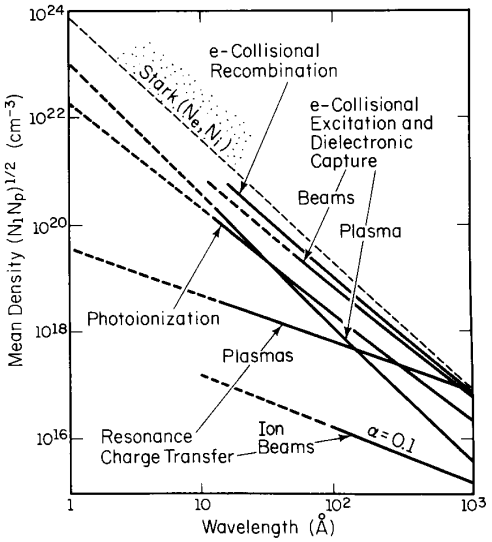

Fig. 1. Wavelength dependence of the mean particle density ($[N_i N_p]^{1/2}$) calculated in [5] to obtain, by selected collisional and optical processes, gains of $\alpha = 5$cm^{-1} ($\alpha = 0.1$cm^{-1} for ion beams). In this graph, N_p denotes the number density of the particle (or photon) responsible for driving the pumping process of interest. For electron impact excitation of a 10-nm laser in a plasma, for example, $(N_i N_p)^{1/2} = (N_i N_e)^{1/2} \approx 10^{18}$cm^{-3}. In the region in which plasma Stark-effect line-broadening dominates, the Stark width scales approximately linearly with the electron (N_e) or ion (N_i) particle number densities. This figure is reprinted from [5] by permission.

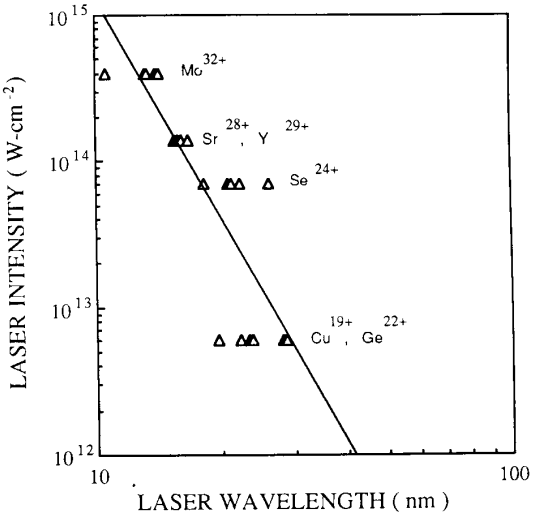

Fig. 2. Peak laser intensities required for pumping various neon-like atomic ion lasers (data after [8]).

TABLE I
XUV AND SOFT X-RAY ATOMIC AMPLIFIERS OBTAINED TO DATE (ADAPTED FROM REFS. [8], [10], AND [11])

Ion	Transition	λ, nm	Laser Intensity, W-cm^{-2} (λ_{laser})	Gain Coefficient (cm^{-1})
		Neon-Like Ions		
Cu^{19+}	3p→3s	22.11, 27.93, 28.47	$6 \cdot 10^{12}$ (1.06 μm)	1.7–2.0
Zn^{20+}	3p→3s	21.22, 26.23, 26.72	—	2.0–2.3
Ga^{21+}	3p→3s	24.67, 25.11	—	—
Ge^{22+}	3p→3s	19.61, 23.22, 23.63, 24.73, 28.65	$6 \cdot 10^{12}$ (1.06 μm)	3.1–4.1
As^{23+}	3p→3s	21.88, 22.26	—	5.4
Se^{24+}	3p→3s	18.24, 20.64, 20.98, 22.03, 26.29	$7 \cdot 10^{13}$ (532 nm)	2.2–4.9
Sr^{28+}	3p→3s	16.41, 16.65	$1.4 \cdot 10^{14}$ (532 nm)	4.0–4.4
Y^{29+}	3p→3s	15.50, 15.71	$1.4 \cdot 10^{14}$ (532 nm)	~ 4
Mo^{32+}	3p→3s	10.64, 13.10, 13.27, 13.94	$4 \cdot 10^{14}$ (532 nm)	2.2–4.2
		Nickel-Like Ions		
Eu^{35+}	4d→4p	6.58, 7.10, 10.04, 10.46	$7 \cdot 10^{13}$ (532 nm)	0.1–1.1
Yb^{42+}	4d→4p	5.03	$1.4 \cdot 10^{14}$ (532 nm)	1.2
		Lithium-Like Ions		
Al^{10+}	4f, 5f→3d	10.57, 15.47	$4 \cdot 10^{12}$– $1.7 \cdot 10^{14}$ (532 nm, 1.06 μm, 10.6 μm)	1.0–3.5
Si^{11+}	4f→3d	12.9	$2 \cdot 10^{13}$ (10.6 μm)	1.5
		Hydrogen-Like Ions		
C^{5+}	3→2	18.2	$5 \cdot 10^{12}$ (10.6 μm), $1.5 \cdot 10^{14}$ (532 nm)	4.1–8.0
F^{8+}	3→2	8.1	$5.7 \cdot 10^{14}$ (532 nm)	5.5

Similar schemes have been developed for inverting XUV and soft X-ray transitions in nickel-like, lithium-like. and hydrogen-like ions. One of the earliest reported soft X-ray amplifiers, based on the hydrogen-like C VI transition at 18.2 nm, was discovered by Suckewer *et al.* at Princeton University [14], [15]. Amplification was observed in a magnetically confined plasma produced by irradiating a carbon disk with ~ 75-ns FWHM, 300-J pulses from a CO_2 laser. As indicated in Table I, single-pass gains exceeding 6.5 were produced on the 3 → 2 transition of the C^{5+} ion upon populating the upper laser level by recombination.

As shown in Table I, the Ni- and Li-like ion systems involve 4d → 4p and nf → 3d (n = 4, 5) transitions, respectively. Hagelstein [16] has recently simulated a prospective laser at ~ 25 nm in nickel-like Mo^{13+}. Electron-impact excitation of the ions's $3d^{10}$ ground state in a plasma having an electron temperature and electron density of 150 eV and $(2 - 4) \cdot 10^{10}\mathrm{cm}^{-3}$, respectively, is expected to result in stimulated emission on the 4d → 4p transition of the ion with predicted peak gain coefficients of ~ $0.06\mathrm{cm}^{-1}$ (at 25.4 nm). Only a few of the possible Li- and H-like ion lasers have yet been demonstrated, and Fig. 3 depicts the range in wavelengths that is available with multiply charged ions having these electronic configurations.

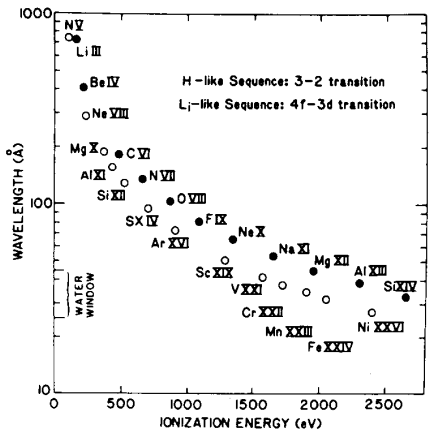

Fig. 3. Variation of the lasing wavelength of hydrogen-like and lithium-like ions with the ionization energy of the ion (reprinted from [17] by permission).

It should be noted that although the fundamental physical processes occurring in these laser systems are presently not thoroughly understood, it is evident that the plasma parameters and n_e and T_e, in particular, are critical to the attainment of gain in this spectral region. Both are, in turn, related

to the target material and peak laser intensity. To a first approximation, the plasma blackbody temperature T is related to the laser intensity I by

$$T \approx 0.6(I\lambda^2)^{2/3} \tag{2}$$

where T, I, and λ are expressed in electronvolts, W-cm^{-2}, and centimeters, respectively. Also, the large optical pump intensities that are necessary to realize gain underscore the validity of Hagelstein's comment that [16] "No one has yet developed an X-ray laser at home in their garage."

At longer wavelengths, Kapteyn *et al.* [18], Silfvast and Wood [19], and Sher *et al.* [20] have demonstrated lasing at 108.9 nm from doubly ionized xenon by photoionizing the neutral ground state directly with $\sim$ 75-eV soft X-ray photons. This photoabsorption process removes an inner-shell 4d electron, producing the $^2D_{3/2,\,5/2}$ state of Xe^+, which subsequently decays by an Auger process to the $5s^0\ 5p^6\ {}^1S_0$ state of Xe III. Both tantalum and gold-electroplated stainless-steel targets were used to produce the soft X-rays, and peak laser intensities ($\lambda = 1.06\ \mu$m) were $2 \cdot 10^{11} - 10^{12}$ W-cm^{-2}. The efficiency for converting 1.06-μm infrared pump power into soft X-ray radiation was estimated to be 2–7% [18], [20], and the blackbody temperature of the plasma was calculated to be 30 eV. Kapteyn *et al.* [18] also found that preventing photons of energy < 50 eV from reaching the Xe gas enhanced the laser output by almost an order of magnitude. Photons below this energy threshold photoionize the atom, but eject a 5s, rather than 4d, electron—thus unnecessarily increasing the electron density without contributing to pumping of the upper laser level. By exciting the Xe III laser in traveling-wave geometry, Sher *et al.* [20] measured a small signal gain of $e^{40}(\gamma_0 = 4.4\ \text{cm}^{-1})$ and single pulse output energies of 20 μJ in the forward direction and 0.4 μJ in the backward direction. The key to making this system practical was the development of a novel, oblique-incidence pumping geometry. Presently, the Xe laser can be effectively pumped with < 500 mJ of 1064 nm (Nd:YAG) radiation and operates at a pulse repetition frequency of 2 Hz. It is anticipated that further development of these techniques will lead to practical sources of even shorter wavelength radiation. The reduced pump energies will permit higher repetition rates (>10 Hz) and result in accessibility of the sources to nonlaser scientists for applications in spectroscopy, imaging, high-resolution holography, nonlinear optics, and materials studies.

In addition to the Xe Auger laser, Silfvast and Wood [19] have reported soft X-ray photoionization-pumped lasers in In^+ at 185 nm and He at 164 nm. Both involve the removal of an inner shell electron, and Fig. 4 shows the energy dependence of the photoionization cross sections of interest for several elements that have lased when pumped by soft X-rays [19].

A *photoelectron*-pumped laser in neutral Cs vapor was recently demonstrated by Barty *et al.* [21]. Although initiated by the production of soft X-rays at a stainless-steel target, this laser is actually collisionally pumped by hot photoelectrons. The conversion efficiency of the $1.5 \cdot 10^{12}$W-cm^{-2}, 1.064-μm pump intensity into soft X-rays was $\sim$ 3%, giving rise to a plasma radiating a $\sim$ 25-eV blackbody spectrum. At this temperature, the photoelectron density is $\sim 10^{16}$cm^{-3} and the

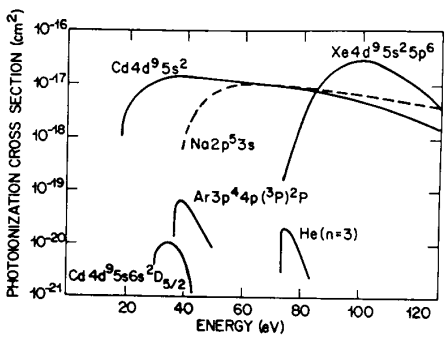

Fig. 4. Dependence of the inner-shell photoionization cross sections on photon energy for several of the atomic lasers reported in [19] (reprinted by permission).

velocity distribution is roughly Maxwellian. Consequently, the excitation rate $\langle \sigma v \rangle$ to the upper laser level—the metastable Cs $5p^5\ 5d\ 6s\ {}^4D_{1/2}$ level—is $3.5 \cdot 10^{-9}$cm^3-s^{-1}, which yields a peak upper state population of $1.2 \cdot 10^{14}$cm^{-3}. Lasing occurred in the extreme ultraviolet at 96.9 nm, and the small signal gain coefficient was measured to be 4.9 cm^{-1}.

Efforts by Rocca *et al.* to produce UV lasers in CW electron-beam-pumped plasmas [22] have yielded 14 mW on the 318.1 nm [$5s\ {}^1G_4 \rightarrow 5p\ {}^3F_3$] transition of the silver ion [23]. Discharge currents exceeding 1 A at 2.5 kV from a two electron-gun arrangement have made it possible to achieve continuous lasing on this and several visible lines of Ag, Zn, Cd, and F by direct electron-impact excitation. In order to improve the specific power loading of the medium and extend the range of available wavelengths into the VUV, Rocca's group is also exploring capillary discharges [24]. Pulsed capillary-confined discharges in He produce electron densities in excess of 10^{17}cm^{-3}, and have the added advantage of rapid plasma cooling by conduction to the discharge cell walls. Strong emission was observed from He II in an effort to obtain gain on its hydrogenic $3 \rightarrow 2$ line. Similar experiments with lithium produced XUV radiation at 72.9 nm from doubly charged Li ions formed in discharges in capillaries fabricated from lithium hydride. Peak current densities up to $2.5 \cdot 10^6$A-cm^{-2} in a 40-kV discharge yielded emission on the $3 \rightarrow 2$ line of Li^{++}, which noticeably intensified in the plasma afterglow, presumably due to pumping of the Li III, n = 3 state by three-body electron–ion recombination in the cooling plasma.

Experiments conducted by Petersen [25] have recently yielded more than 80 new CW lasing lines from ionic transitions of the rare gases. With a $\sim$ 2.6-mm bore, but otherwise conventional ion-laser plasma tube, he reported continuous lasing on 46 lines in the 200–300 nm region, and 43 in the 300–400 nm interval. Most exhibited threshold currents of 40–70 A (730 – 1280A-cm^{-2}), which is a reflection of the fact that the upper levels for these laser transitions lie as much as 125 eV above the ground state for the neutral species. Single-line output powers up to $\sim$ 0.65 W have been obtained, and, for Kr, the output power for all the lines in the 242–266 nm region was 2.5 W. In Ar, the lasing transitions in the 275–306 nm range yielded as much as 6 W of CW power.

B. Molecular Lasers

The introduction of new UV and VUV molecular lasers over the past several years has slowed considerably as emphasis has shifted to the development of existing systems, and to the F_2 laser, in particular. Recent experiments conducted by Yamada *et al.* [26] increased the output pulse energy of this laser by almost an order of magnitude over previous devices (to beyond 100 mJ/pulse). Improvements in the laser's extraction efficiency were attributed to a reduced anode–cathode gap (and, hence, increased E/N) and the use of diluent pressures as high as $\sim$ 6000 torr ($\sim$ 8 atm). Modeling of this system by Kim *et al.* [27] and Ohwa and Obara [28] bear out these results. Efficient operation of the laser requires specific power loadings of the active medium in the $\sim 4 - 23$ MW-cm^{-3} range [26], which is roughly an order of magnitude larger than that required for the rare gas–halide systems. This, of course, is a reflection of the large ionization potentials of both of the constituents of the F_2 laser gas mixture (He, F_2). For a He/F_2 (99.85/0.15%) gas mixture at a total pressure of 2.6 atm, for example, Ohwa and Obara [28] calculate the electron temperature to be 4.6 eV for $E/N = 7.7 \cdot 10^{-17}$V-cm^{-2}.

The higher power deposition requirements for the F_2 laser stem not only from the higher power deposition inherent with high-pressure operation, but also from several kinetics factors. Simulations [28] suggest that the acceleration in the removal rate for the laser's lower level [$F_2(A')$] population and temporal broadening of the laser pulse are critical issues favoring increased background pressures. Consequently, to obtain intrinsic laser efficiencies exceeding 1% requires total gas pressures of at least 4 atm [28]. Similar conclusions were reached by Kim *et al.* [27].

The F_2 laser has been developed to such an extent that commercially available systems now offer several watts of output power at pulse repetition frequencies exceeding 50 Hz. While the gas lifetime is below 10^6 shots, continuing improvements in laser-head construction materials and design promise to extend the gas-fill lifetime and improve single-pulse output energies by at least a factor of two.

A striking example of the utility of laser-produced plasmas in pumping molecular lasers by electron impact is the H_2 VUV laser experiments reported by Benerofe *et. al.* [29]. Molecular hydrogen was photoionized with soft X-rays produced by a traveling-wave laser plasma. When the plasma is produced by $\sim$ 580 mJ, 200-ps pulses from an Nd:YAG laser, free electrons generated by the photoionization process have an average energy of 10 eV, and the electron density is estimated to be $3 \cdot 10^{15}$cm^{-3} in the active volume. Figs. 5(a) and (b) compare the photon energy distribution for a 12-eV blackbody with the H_2 photoionization cross section. The electron energy distribution calculated in [29] is illustrated in Fig. 5(c) and, Fig. 5(d) shows the H_2 $C^1\pi \leftarrow X^1\Sigma_g^+$ (Werner band) electron-impact, excitation cross section. With this pumping technique a gain coefficient of 0.9 cm^{-1} was measured at room temperature for a gain length of 27 cm. Lowering the gas temperature to 100 K results in the gain coefficient rising to $\sim$ 1.5 cm^{-1}.

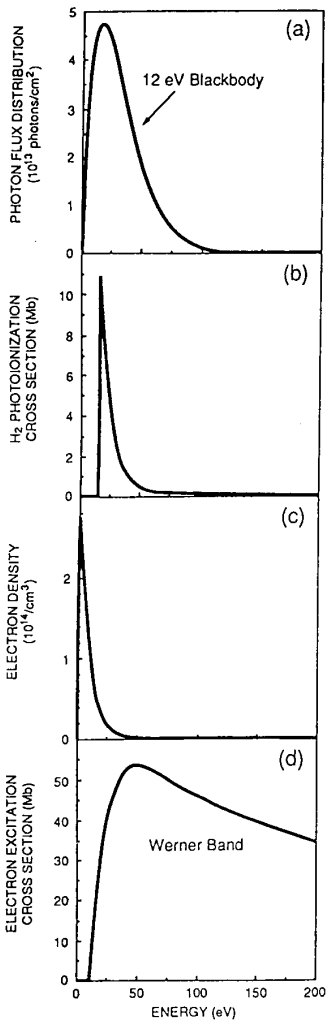

Fig. 5. Data relevant to the operation of the H_2 116-nm laser pumped by a photoionization electron source. Comparison of: (a) the photon energy distribution emitted by a 12-eV blackbody, (b) the H_2 photoionization cross section, (c) the calculated electron density, and (d) the electron-impact excitation cross section for the Werner band (C←X) of H_2 (reprinted from [29] by permission).

C. Future Prospects

Since the single-pulse energies and repetition rates available with a transverse discharge-pumped F_2 laser exceed those from other sources in the VUV, near-term efforts will undoubtedly focus on further improving the efficiency of this laser. However, since the $D' \rightarrow A'$ lasing transition in F_2 occurs between two bound states, the tunability of this system is limited and the development of primary sources in the VUV (or XUV for that matter) that are tunable would be extremely valuable for several applications, including spectroscopy, optical imaging, and materials analysis. Toward that end, Sauerbrey and Langhoff [30] have proposed and explored the excimer (bound $\rightarrow$ free) transitions of the singly charged alkali–halide ions as possible VUV laser-active media. Following the trend toward higher stages of ionization in atomic systems, increased attention to

ionized small molecules seems inevitable in order to satisfy the competing requirements of tunability and short wavelength.

For the laser plasma-pumped atomic lasers, increased efforts in the optical properties of materials in the VUV, XUV, and soft X-ray spectral regions and the application of MBE and MOCVD film-deposition techniques to multilayer fabrication will lead to steady improvements in the performance of short-wavelength optical components. A major impediment in the past to progress has been the quality of available optics, but the plenary paper given at CLEO'91 by R. Freeman of Bell Laboratories highlighted the advances that have been realized recently in the fabrication of reflective optics in the soft X-ray region. Improvements in the interfacial quality of multilayer structures have yielded reflectivities exceeding 60–70% at 130 nm, for example. Over the next five years, one can expect even greater strides to be taken in this area, which will translate into soft X-ray oscillators that have higher peak powers and yet are more compact. Coupled with more widespread use of the traveling-wave excitation technique developed at Stanford, such advances will lower threshold pumping powers, bringing these atomic lasers within the financial reach of more laboratories. Improvements in target design so as to more efficiently convert near-IR or visible laser power into soft X-rays of the desired energies will encourage this trend.

III. Visible and Near-UV Lasers

Infrared lasers which operate on transitions between vibrational levels of the lowest electronic state have upper levels which are at most a few tenths of an electronvolt above the ground level. As a result, gas discharges can be easily constructed which have characteristic energies commensurate with these values. Visible and near-UV lasers, however, operate on electronic transitions whose upper laser level is a few to 10's of electronvolts above the ground state. It is difficult, particularly on a CW basis, to construct gas discharges which have these characteristic energies. As a result, visible and near-UV (VNUV) lasers usually rely on a fortuitous sequence of kinetic processes to excite the upper laser level. For example, many metal ion lasers are excited by excitation transfer from an electronically excited noble gas atom whose levels fortuitously align themselves with the appropriate levels in the metal atom. For example, in the Cd^+ laser, the upper levels are produced by excitation transfer from helium metastable atoms,

$$\mathrm{He}(2^1\mathrm{S}, 2^3\mathrm{S}) + \mathrm{Cd}(^1\mathrm{S}_0) \rightarrow \mathrm{Cd}^+(5\mathrm{s}^2\,{}^2\mathrm{D}_{5/2}) + \mathrm{He}(1^2\mathrm{S}_0) + \mathrm{e}. \quad (3a)$$

Laser oscillation then follows on the 441.6-nm transition

$$\mathrm{Cd}^+(5\mathrm{s}^2\,{}^2\mathrm{D}_{5/2}) \rightarrow \mathrm{Cd}^+(5\mathrm{p}^2\,{}^2\mathrm{P}_{3/2}) + \mathrm{h}\nu(2.8\mathrm{eV}). \quad (3b)$$

Gas discharges used for VNUV lasers therefore tend to be somewhat specialized, each being designed to persuade the energy flow to follow a certain kinetic pathway which enables threshold to be reached. For example, at one end of the extreme are excimer lasers (193–351 nm) which are excited by pulsed gas discharges having pulse lengths of 10–100 ns, gas pressures of 1–5 atm, and a power deposition of 100 kW-cm^{-3} to a few MW-cm^{-3}. At the opposite end of the category are He–Ne lasers which operate on a CW basis at gas pressures of a few torr and power depositions of a few to 10's W-cm^{-3}.

Due to the specialized nature of gas discharges for VNUV lasers, it is difficult to present a general discussion of their properties. This uniqueness is illustrated by discussing how gas discharges may be designed to enhance certain plasma–chemical attributes which, in this case, result in laser oscillation. In this section we will discuss excimer lasers as an exemplary system of how the gas discharge may set limits on the performance of the laser.

A. General Properties of Excimer Lasers

Electric discharge excimer lasers provide highly efficient sources of pulsed coherent ultraviolet (UV) radiation [31]. The term "excimer" has now come to refer to a class of excited molecules which are bound in their excited states, and repulsive or weakly bound ($D_0 \leq kT$) in their ground states. Laser transitions typically occur between the lowest excited states of these molecules and their ground states. These molecules thereby constitute nearly ideal laser media. Since their ground states are unstable, inversions are readily obtained by pumping the upper level. Transitions to the ground state then result in dissociation of the molecule. The fact that their ground states are not stable, though, means that excimer species themselves cannot be feedstock gases and must be generated "real time" in the plasma. Excimer lasers are therefore accurately described as "plasma–chemical" lasers.

A variety of excimer molecules have demonstrated laser action. The most successful in terms of efficiency, laser energy, and technological development are the rare gas halogen (RgH) excimers. The RgH lasers that have been most intensively developed are ArF (193 nm), KrF (248 nm), XeCl (308 nm), and XeF (351 nm). The excited RgH excimer results from the ion pair consisting of the rare gas (Rg) positive ion and the halogen (H) negative ion. (See Fig. 6.) These excimer lasers typically operate between the bound B state of the ion pair and the repulsive (or weakly bound) X state. The B→X transitions have wavelengths ranging from 192 nm for ArF(B→X) to 351 nm for XeF(B→X). Visible wavelengths can be obtained by operating on the lower gain (C→A) transitions of the XeCl and XeF molecules.

A schematic of a typical discharge laser appears in Fig. 7 [31]–[33]. The electrode separation is a few to 10 cm, with lengths of 10's of cm to > 1 m. The gas pressure is 1–5 atm (see below). The discharge circuit consists of a pulse-forming line (PFL) with electrical lengths of 10's to 100's of ns. The charging voltage of the PFL is 1–4 kV/cm-atm, resulting in a power deposition of 100 kW-cm^{-3} to many MW-cm^{-3}. The voltage is switched onto the laser head using a thyratron or low-inductance rail-gap switch, causing breakdown and sustaining a discharge current of 100's of A-cm^{-2}. The impedance of the discharge is typically 0.1–0.5 Ω-m based on a square aperture. Variants of the discharge circuit use saturable magnetic inductors [35] to aid in switching, or a separate "spiker" circuit to breakdown the gas [36], thereby allowing better impedance matching between the sustainer PFL and laser head. It is mandatory that the discharge volume

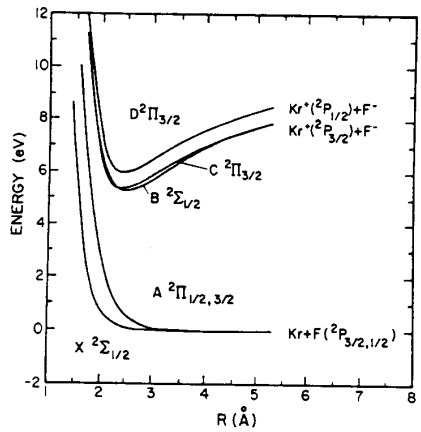

Fig. 6. Energy levels of the KrF exciplex. Laser oscillation at 248 nm takes place on the B→X transition [31].

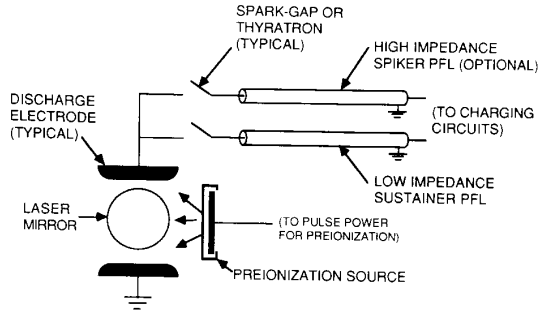

Fig. 7. Schematic of a discharge-excited excimer laser. The discharge electrodes are typically separated by a few to 10 cm and have lengths of 10's of cm to 1 m. The optical axis is parallel to the long dimension of the electrodes.

be uniformly preionized to $10^7 - 10^8 \mathrm{cm}^{-3}$ prior to applying high voltage. Preionization is accomplished using UV spark arrays [37], X-rays [38], [39], and corona bars [40].

Commercial excimer lasers are currently available which deliver a few joules of pulse energy at repetition rates of 100's of Hz, yielding as much as 500 W [41]. The discharge apertures on these devices are a few centimeters, wallplug efficiencies are a few percent, and the laser pulse lengths are usually $\leq$ 30 ns. Higher pulse energies ($\leq$ 66 J) [42], [43], larger apertures ($\leq$ 20 cm) [43], higher efficiencies of ($\leq 4\%$) [44], and longer pulse lengths of ($\leq 1.5\ \mu$s) [37] have been obtained with XeCl laboratory lasers, although not all on a single device.

Excited states of the RgH exciplex are typically generated via an ion–ion neutralization process constituting the ion channel, or a harpooning reaction constituting the neutral channel. For purposes of discussion we will use the KrF laser in Ar/Kr/F2 and He/Kr/F2 mixtures as a model system. The processes discussed for KrF are directly analogous to other RgH systems. For example, the KrF(B) molecule is formed through the ion channel by [44], [45]

$$\mathrm{Kr}^+ + \mathrm{F}^- + \mathrm{M} \rightarrow \mathrm{KrF(B, v)} + \mathrm{M} \tag{4}$$

$$\mathrm{Kr}_2^+ + \mathrm{F}^- + \mathrm{M} \rightarrow \mathrm{KrF(B, v)} + \mathrm{Kr} + \mathrm{M} \tag{5}$$

where M is a stabilizing third body. The neutral channel consists dominantly of harpooning reactions, exemplified by [46]

$$\mathrm{Kr}^* + \mathrm{F}_2 \rightarrow \mathrm{KrF(B, v)} + \mathrm{F} \tag{6}$$

where Kr^* represents Kr in an excited state. As argon is often used in the gas mixture for a KrF, additional excitation reactions such as

$$\mathrm{ArF(B)} + \mathrm{Kr} \rightarrow \mathrm{KrF(B, v)} + \mathrm{Ar} \tag{7}$$

are possible where the ArF exciplex was previously formed by reactions analogous to those shown above. These formation reactions are exothermic by a few to many electronvolts, resulting in KrF(B, v) being formed high in the vibrational manifold. Lasing, however, occurs out of KrF(B, v=0). Therefore collisional relaxation of the vibrational manifold must occur before lasing [47].

B. Scaling Considerations

The formation efficiency (power channeled to the upper laser level compared to power deposited in the plasma) of KrF excimer lasers may be as high as 40%. This high efficiency results from the fact that with the exception of the repulsive A states of the F_2 molecule (which has a small mole fraction anyway), the upper laser level is energetically the lowest excited electronic state in the system. Therefore power deposited in the plasma will naturally channel by excitation transfer down to the upper laser level [48]. For example, suppose an Ar^+ is produced by an electronic-impact collision. Dimerization rapidly follows, after which charge transfer produces Kr^+. This reaction is followed by an ion–ion neutralization which produces the upper laser level:

$$\begin{matrix} & \mathrm{Ar} & & \mathrm{Kr} & & \mathrm{Kr} & & \mathrm{F}^- & \\ \mathrm{e} + \mathrm{Ar} \rightarrow & \mathrm{Ar}^+ & \rightarrow & \mathrm{Ar}_2^+ & \rightarrow & \mathrm{Kr}^+ & \rightarrow & \mathrm{Kr}_2^+ & \rightarrow \mathrm{KrF(B)}. \end{matrix} \tag{8}$$

Gas mixtures for excimer lasers are usually tertiary, containing a lower atomic weight noble gas in addition to the rare gas and halogen for the excimer molecule. For example, in discharge-excited KrF lasers a typical gas mixture is $He/Kr/F_2$ = 99.5/0.5/0.05. Although binary gas mixtures (e.g., Kr/F_2) have been investigated, optimum performance is usually obtained with a tertiary mixture. The tertiary mixture is necessary due to the large momentum-transfer cross section of the Rg which forms the exciplex. The cross sections for electron-impact momentum transfer σ_m for Ar, Kr, and Xe exceed 10 A^2 for energies in the range of 5–10 eV [49].

These values of σ_m would require excessively high operating and breakdown voltages for large aperture discharges (greater than a few centimeters). Therefore the average σ_m mixture must be reduced by diluting with either He or Ne, both of which have lower momentum transfer cross sections compared to the heavier rare gases. In practice, avalanche-discharge excimer lasers (pulse lengths <20–30 ns) tend to use He as a buffer gas. Long-pulse ($\geq$ many 10's ns) discharge

excimer lasers tend to use Ne as a buffer gas, since its lower momentum transfer cross section at energies $\leq$ 10 eV is advantageous.

The requirement that excimer lasers must operate at pressures exceeding an atmosphere results from the fact that the formation of the upper laser level through the ion channel requires a three-body reaction in order for its rate to be competitive with other excitation or quenching processes. For example, the rate constant for ion–ion neutralization resulting in atomic products,

$$Kr^+ + F^- \rightarrow Kr + F. \quad (9)$$

$k_g \approx 10^{-7} - 10^{-6} cm^3 s^{-1}$ [50]. The ion–ion neutralization reaction resulting in formation of the exciplex dimer is a three-body reaction [44], [45]:

$$Kr^+ + F^- + M \rightarrow KrF(B) + M \quad (10)$$

where M is any third body and is required to conserve momentum. In order for the exciplex-forming reaction to effectively compete with the neutralization reaction, the density of the third body must be $[M] \gg k_g/k_{10}$. Although there is a complicated dependence of k_{10} on [M], over the range of 0–3 atm, $k_{10}[M = Ar] \approx 3 \times 10^{-6} cm^3 s^{-1} atm^{-1}$ [39]. Therefore the total gas pressure must exceed an atmosphere in order for the reaction (10), which forms the exciplex, to dominate.

Due to the efficiency with which deposited power is channeled to the upper laser level, the characteristics of laser operation are largely a function of local power deposition. Therefore the manner and uniformity of power deposition is often the greatest concern in constructing the device and optimizing laser performance [34], [51]–[54]. The uniformity of power deposition is largely determined by the distribution of the preionization density. Since near its optimum value, laser efficiency is relatively insensitive to small changes in other parameters such as gas mixtures, power deposition is the only remaining parameter which may be optimized and which characterizes the laser. For example, in discharge-excimer lasers, discharge instabilities limit power deposition and constrain laser performance, as opposed to being a limiting aspect of the kinetics.

From past experience and simple scaling laws one could recommend that excimer lasers be operated at low-power deposition to enhance their discharge stability. The short radiative lifetime of the upper laser level, however, sets stringent requirements on pump rate and gas pressure. For example, the radiative lifetime of the rare gas–halide excimers B state ranges from 6 ns for KrF to 15 ns for XeF [31]. When also considering quenching processes, the total lifetime τ_t of the B state is 50–70% of the radiative value. The short lifetimes of these molecules sets a requirement on the rate of pumping of the medium. For example, for power deposition P (W-cm^{-3}) and formation efficiency η_f, the unsaturated density of the upper laser level is $N_u = \eta_f P \tau_t / h\nu$, where $h\nu$ is the laser photon energy. To obtain a specific small signal gain, $g_0(cm^{-1})$, the power deposition must be

$$P \approx g_0 h\nu / \sigma_e \eta_f \tau_t \quad (11)$$

where σ_e is the optical stimulated-emission cross section. Since the excimer transition is essentially bound-free, the optical emission cross section tends to be small compared to that for atomic bound–bound transitions. For example, the optical stimulated-emission cross section for KrF is $2.6 \times 10^{-16} cm^2$ [31], which combined with a formation efficiency of 25% and effective lifetime of 5 ns, the power deposition in a KrF laser must be 250 kW-cm^{-3} to obtain a small signal gain of 0.1 cm^{-1}. With this power deposition, the system must be operated on a pulsed basis.

The fact that high-power deposition is required sets further limits on the gas pressure. Power deposition in an electric discharge is given by $P = j_d E_s$, where j_d is the discharge current density and E_s is the self-sustaining electric field. The self-sustaining electric field is determined almost entirely by the gas mixture. It is that value where

$$\Sigma_j f_j k_{Ij} = \Sigma_j f_j k_{aj} \quad (12)$$

where f_j is the mole fraction of component j, k_{Ij} is its ionization rate coefficient, and k_{aj} is its attachment rate coefficient. For typical lasers $E/N \approx 2 - 5$ Td (1 Td = 1×10^{-17} V-cm^2) [33], [35] or $E/p \approx 0.4 - 1.0$ kV/cm-atm. The current density is $j = E_s n_e e^2/(m_e \nu_m)$ and in typical gas mixtures, $\nu_m = 2 \times 10^{12}$ p(atm) s^{-1}. These values result in $j_d \approx 3.5 \times 10^3 E_s$ (kV/cm-atm) p(atm) f kA-cm^{-2}, where f is the fractional ionization. Power deposition in an excimer laser discharge is therefore:

$$P(kW\text{-}cm^{-3}) \approx 3.5 \times 10^6 E_s^2 (kV/cm\text{-}atm) p^2(atm) f. \quad (13)$$

Since discharge lasers typically operate with fractional ionization of 10^{-6} to 10^{-5}, to obtain power depositions of 100's kW-cm^{-3} the gas pressure must be at least a few atmospheres.

C. Uniformity and Instabilities

The purpose of the discussion above is to motivate the reader to view discharge-excited excimer lasers as systems whose performance depends primarily on local power deposition. The details of the kinetic processes leading to excitation of the upper laser level bracket the specific gas pressure and power deposition which are required. To the extent that excimer lasers are power-driven devices, their performance is typically limited by issues relating to power deposition as opposed to any particular kinetic mechanism. For example, the laser pulses in electric discharge-excited excimers are usually terminated by discharge instabilities (e.g., arcing, constriction, streamers) which prevent the gas from being uniformly excited rather than bottle-necking in the kinetics. These discharge instabilities, which develop on time scales of 10's to 100's of nanoseconds, originate from a nonuniformity in gas mixture, preionization, density, or electric field (resulting from electrode contouring).

To examine the limiting aspects of discharge stability on the performance of excimer lasers it may be useful to view the plasma as simply a network of nonlinear resistors. Since excimer lasers are typically transversely excited, the plasma may be logically divided into segments which are perpendicular to both the electrodes and the optical axis, thereby making

a parallel array. The conductivity of each segment σ_i and the total conductivity of the discharge σ are

$$\sigma_i = (A/l)_i(nq^2/m_e\nu_m)_i, \quad \sigma = \Sigma_i\sigma_i \tag{14}$$

where l is the length of the segment, A is its cross-sectional area, n is the electron density in the segment, and ν_m is the electron momentum-transfer collision frequency. The power deposition in a particular segment is therefore:

$$P = j_iE_i = \sigma_iE_i^2 \propto n_i. \tag{15}$$

If we limit ourselves to plane parallel electrodes, the E/N across each plasma segment is the same. The relative power deposition between segments therefore scales to first order as the ratio of their electron densities. Instabilities resulting in largely disparate power deposition must then have originated from processes which cause or reinforce small changes in electron density.

In excimer lasers, where electron loss is dominated by attachment to the halogen donor (e.g., F_2 in a KrF laser) and in which the halogen donor is consumed during the discharge pulse, small changes in the initial preionization electron density can lead directly to constriction and arcing. Under quasi-steady-state conditions the local self-sustaining electric field is determined by a balance between ionization and electron loss, in this case attachment. The operating point of the discharge is then the value of E/N which satisfies (12). The mole-fraction-weighted rate coefficients for ionization and attachment are functions of halogen density, excited-state density, and electron density, in addition to being functions of E/N. Therefore the operating point in a discharge may vary as a function of position as these parameters also are spatially varying.

An instability will occur, because when the operating points of various segments of the discharge are different, the discharge cannot operate at all of those points simultaneously. Since the operating point E/N will be highest where the halogen density is largest, then there will be an ionization excess at locations where the halogen density is lower. The electron density thereby increases in those plasma segments. If the halogen donor is consumed by the attachment process (e.g., $e + F_2 \rightarrow F^- + F$) and is not replenished during the discharge pulse, then the rate of burnup of the halogen also increases, leading to a higher electron density and further burnup. This process is unstable and will eventually lead to arcing.

The rate-limiting process of the performance of a discharge-excited excimer laser is therefore the uniformity of power deposition. The uniformity of power deposition is determined by the uniformity of the preionization density, electric field, and reactants (e.g., halogen density) which may cause the operating point of a given plasma segment (that is, its local self-sustaining E/N) to be different from that provided by the discharge. The degree of nonuniformity which may be tolerated is quite small. To demonstrate this effect an electric discharge KrF(B→X) laser has been modeled. This simulation includes rate equations for the heavy particle and electron collisions, and also includes models for the external electrical circuitry and laser extraction. The model is a time-dependent one-dimensional representation and is based on models described in [35] and [55]–[57]. The experimental conditions for this demonstration are those of Watanabe and Endoh [33]. The device uses a $He/Kr/F_2$ = 99.47/0.44/0.09 gas mixture at 4.5 atm. The discharge active volume is 7 x 7 x 80 cm^3. An intrinsic laser-energy efficiency of 1.2% was obtained with an output energy of 10 J. The experimental and theoretical current and voltage waveforms are shown in Fig. 8.

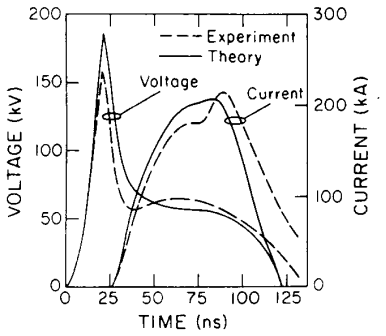

Fig. 8. Experimental and theoretical waveforms for the discharge-excited laser constructed by Watanabe and Endoh [33].

An instability can result from a nonuniformity in electric field, preionization electron density, or gas mixture which results in nonuniform halogen burnup. A common source is nonuniformities in preionization electron density. To demonstrate this effect we have varied the preionization density profile in the discharge KrF laser. Power deposition at the end of the current pulse is shown in Fig. 9 for fractional edge-to-center nonuniformities in a preionization density of 0–0.1 (highest on axis). The spatial dimension in the figure is parallel to the electrodes and perpendicular to the optical axis. In all cases, power deposition at the leading edge of the discharge pulse is fairly uniform as a function of position and no worse than in the ratio of the preionization density. At these early times the F_2 concentration has not been significantly depleted so that all spatial locations have the same E/N operating point. As the F_2 is gradually depleted more rapidly near the axis where the preionization density is the highest, the stable operating point at those locations decreases to a value smaller than the average E/N, thereby creating an ionization excess. An electron avalanche is then initiated, resulting in more rapid depletion of F_2. This results in constriction of the discharge and termination of laser oscillation.

Another effect which can cause an instability is E/N not being uniform, which may occur as a result of nonaligned electrodes. To demonstrate this effect we varied the alignment of the electrodes to cause an edge-to-center fractional change in E/N of 0–0.01 (highest on the axis), while keeping the preionization density uniform. These results are shown in Fig. 10. Only small variation ($\ll 0.1\%$) changes in E/N can be tolerated before constriction of the discharge and termination of laser oscillation occurs.

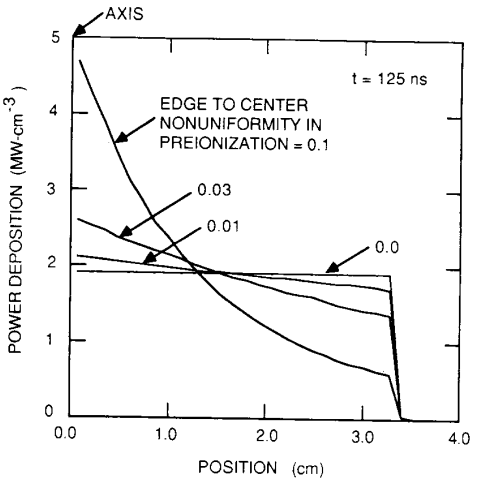

Fig. 9. Power deposition at the end of the current pulse when the preionization density has a fractional edge to the center nonuniformity of 0.1 (highest on the axis).

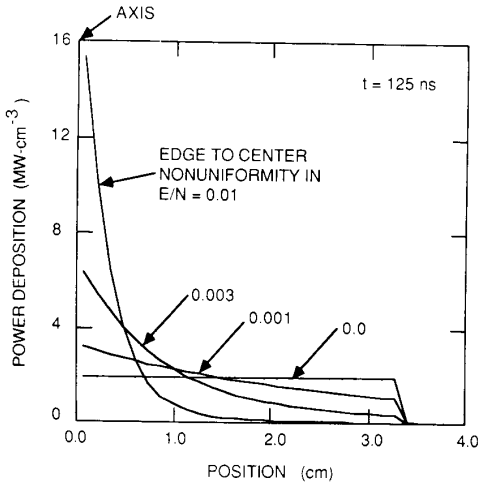

Fig. 10. Power deposition at the end of the current pulse when the applied electric field has a fractional edge-to-center nonuniformity of 0.01 (highest on the axis).

IV. Infrared Molecular-Gas Lasers

A. Introduction

Infrared lasers generated by electrical discharges in molecular gases must satisfy three principal requirements if they are to be efficient and useful. First, the discharge must excite certain vibrational modes efficiently. These can be the vibrational modes of the lasing species or of donor molecules. In terms of the gas-discharge parameters, this means that selection of the mean electron energy is accomplished by control of the E/N parameter. One attempts to optimize the overlap between the EEDF (electron energy distribution function) and the excitation cross sections. Secondly, the plasma chemistry induced by the discharge should not change the composition of the gas mixture too rapidly, or alternatively the system should allow for these changes. In practical situations this usually means that dissociation processes should not severely deplete the lasing molecule density and the products should not quench the lasing species. Therefore E/N should not be too high and the discharge should not provide many energetic electrons capable of causing dissociation. If the new species formed have large attachment rates, this can lead to a macroscopic discharge instability. The third feature is that the temperature of the gas mixture must not be allowed to become comparable to the energy of the lower level; otherwise thermal pumping of this level will prevent the population inversion. Heating of the gases occurs due to vibrational–rotational to translational energy transfer from excited vibrational states (including those whose populations are increased by lasing), and to a lesser extent by electron molecule elastic collisions.

TABLE II
Time Constants(s) of Energy Relaxation Processes in Molecular Gas Discharges.

Space-charge relaxation	10^{-10}–10^{-9}
Electron energy relaxation	10^{-9}–10^{-7}
Ionization and attachment	10^{-7}–10^{-5}
Vibrational relaxation	10^{-4}–10^{-2}
Thermal energy diffusion	10^{-4}–10^{-2}
Gas residence time	10^{-3}–10^{-1}
Plasma chemistry	10^{-6}–10^{0}

Depending on the boundary conditions, several of these effects can be occurring simultaneously. A summary of the estimated time constants for the principal phenomena in these discharges is given in Table II. Some of the important lasers and the range of lasing transitions are listed in Table III.

The molecules CO_2, N_2O, OCS, CS_2, and HCN are linear triatomics, and all have two stretching vibrational modes and a bending mode. The CO_2, N_2O, and CS_2 systems can be excited directly in discharges and also have operated by energy transfer from vibrationally excited nitrogen. The OCS transitions around 8.25 μm appear in high-current pulsed discharges at low pressures. Various HCN transitions occur in pulsed and/or CW discharges from HCN or a variety of precursors such as CH_4 and NH_3/N_2 or CH_3CN.

The fortuitous near-coincidence of the vibrational energy levels of N_2 ($v = 1$) and CO_2 (001) and the consequent high efficiency of this laser have led to a dominance of research on the CO_2–N_2–He laser among infrared lasers [58]. The highest efficiency laser ($\sim$ 50%), summing over all lasing lines, is the carbon monoxide laser, which also depends on vibrational excitation. This high efficiency is achieved in CO, because an absolute population inversion is not required and, under appropriate conditions, there is fast redistribution of the vibrational energy by anharmonic pumping [59]. Also, multiple wavelength cascade lasing from levels as high as $v = 37$ to $v = 36$ down to the $v = 1$ to $v = 0$ transition can occur.

The characteristic energies involved in the infrared lasers determine the operational parameters. The 5- and 10-μm wavelengths correspond to approximately 0.2- and 0.1-eV transitions, respectively. The ionization energies of the lasing

TABLE III
PRINCIPAL TRANSITIONS IN MOLECULAR GAS DISCHARGE IR LASERS.

Molecule	Wavelength Range (μm)	Important Lines
CO	4.9–6.66	5.263, 5.203
DBr	5.8–6.33	6.19, 6.224
DCl	5.04–5.6	5.15, 5.18
DF	3.83–4.02	2.71, 2.76, 2.83
H_2	0.835–1.3	1.12, 1.30
HBr	4.0–4.65; 19.4–23.4	4.2, 4.46, 4.57
HCl	3.7–4; 13.9–19.8	3.84
HF	2.64–3.05; 10.2–21.8	2.83
N_2	0.75–8.2	0.87, 0.9
CO_2	4.32–4.38; 9.12–17.4	10.6
D_2O	26.4–218.5	33.9, 35.1
H_2O	2.28–67.2	79, 90
H_2S	33.48–225	162, 225
HCN	12.85–773	337
N_2O	10.34–11.04	10.5, 10.9
SO_2	10.85–215.3	140.85
OCS	8.24–8.42; 123–132	—
CH_3I	3.04	—

species are approximately 15 eV, and the electron-impact dissociation energies are in the range of 6 to 10 eV. The direct vibrational excitation energies are 0.3 eV, and the much more important resonant vibrational-excitation energies typically are 2 to 4 eV. Thus, one aims to maintain an EEDF that provides vibrational excitation and sufficient ionization to sustain the power loading into the discharge, but not too high an average electron energy, otherwise dissociation is rapid. There are various methods by which these constraints can be satisfied. Under low-pressure nonflowing conditions, one can add a gas with a low ionization potential and a large cross section for ionization. Xenon satisfies these requirements and does not participate in the chemistry of the discharge. Alternatively, at higher pressures the ionization can be supplied by external sources such as high-energy electron beams [60].

Gas heating constraints can be alleviated by either boundary cooling, precooling, or gas flow and expansion methods. These methods will be discussed further below. In the case of the carbon monoxide laser, cryogenic cooling is required for sealed-off, low-vibrational transition lasing. The low gas temperature reduces the competition of vibrational–translational collisions with vibrational–vibrational energy exchange.

Discharges in complex molecular gas mixtures had been studied for many years and empirical observations on the phenomenology had been made on electronegative gases [61]; for example, the ionization forms in oxygen-rich discharges and the onset of constrictions [62] in gas mixtures. However, this body of work was not generally useful in laser development. First of all, the investigators did not work with gas mixtures of particular interest to lasers; they rarely used flowing gases and so had little or no control on the gas chemistry; and finally, considerably more research was concentrated on the unstable forms of the discharge, rather than attempting to extend the regimes of uniform plasma operation. Assistance to the development of laser physics came primarily from the knowledge of cross sections [60], the collisional processes involved, and the theoretical infrastructure for the calculation of electron energy distribution functions and energy deposition in gases.

B. Specific Molecular Laser Processes

Research in gaseous electronics and gas discharge physics actually had indicated the possibility of laser action in molecular gases very early, but the clues were not pulled together until Patel's experiments. In his book *Electrons in Gases*, Sir John Townsend [64] noted that there is a large increase in electron-energy losses in collisions with N_2 molecules above a mean energy of 0.8 eV. Reviewing data obtained in 1929, he wrote: "In N_2 it must be assumed that in the experiments on the determination of the mean energy and drift velocities, there are losses of energy in large amounts in some of the collisions of the electrons with atoms of nitrogen where the value of E/P is 20, and the mean energy of the electrons is 2.2 eV." In this quote the word "atoms" is used in the generic sense to mean atoms or molecules. It must be remembered that it was not readily apparent at that time how an electron collision in nitrogen could cause vibrational excitation efficiently or why it would require 2.3 rather than 0.3 eV, the vibrational mode energy. Thus the understanding of the efficient vibrational excitation of nitrogen lay dormant until the temporary negative ion mechanism was identified (cf. [65]).

A large number of molecular gas-laser transitions in various gases have been shown to be possible using discharge or discharge-assisted excitation [66]. Only the higher efficiency and noncorrosive systems have received concentrated attention and full investigation. There are many reports of different lines lasing under rather specific excitation conditions. However, for many gases these systems are specialized, offer low efficiency, or do not show much promise of volumetric or power scaling. The results were of interest primarily for the spectroscopic information that they provided. There is an approximate correlation between the energy of the laser transition and the electron-impact dissociation energy of the gas. This means that at longer wavelengths the gas is very easily dissociated. Eventually, for rotational transitions it is more appropriate to use optical pumping.

The first proposal for molecular gas-infrared lasers appears to be that of Polanyi [67], and the discovery of laser action in a pulsed gas discharge (in nitrogen) was reported by Mathias and Parker in 1963 [68]. Fast energy-transfer processes between N_2, CO, and CO_2 had been appreciated for many years by the shock tube community. There is an interesting discussion in the *Proceedings of the 12th Solvay Institute Chemistry Conference*, where Hornig *et al.* [69] discuss the close coupling between vibrationally excited nitrogen and CO or CO_2. In fact, the very fast relaxation of CO_2 by water vapor is also mentioned. Continuous wave operation (at 1 mW) in CO_2 was first

announced by Patel [70], with excellent descriptions of the lasing mechanism and transitions involved. Improvements in power output came with the addition of nitrogen (initially as a mixing laser). The nitrogen N_2 ($v = 1$) level is easily excited via a temporary negative ion resonance, and it rapidly transfers energy to the CO_2 (001) asymmetric stretch vibration. The addition of helium to the mixture gave further improvements (now at levels up to 100-kW CW). The helium assists in maintaining low gas temperature and also increases the relaxation rate of the lower level. Scaling of the laser power has occurred in gas density, volume, and energy loading. The related problems in discharge physics were primarily to avoid the glow-to-arc transition and to provide sufficient gas cooling.

C. Low-Energy Lasers

The scaling laws for positive-column-dominated gas discharges at low pressures and at low input power were developed in the 1920's and 1930's. They were assembled in the landmark book by von Engel and Steenbeck in 1934 [71] and later reviewed by Francis [72]. While these similarity laws appeared to be useful in application to helium–neon laser discharges, the higher power densities of molecular gas lasers necessitated revisions. Abrams and Bridges [73] updated these relationships for laser discharges (cf. Table IV), using the revisions provided by Konyukhov [74]. These allow for the high-power densities of the laser discharge and the consequent gas heating. Konyukhov noted that if molecular gas discharges of different diameter have the same gas temperature and electron temperature, they obey similarity rules (not quite the same as atomic gases) with consequent relations that apply to laser gain and efficiency. At the higher gas pressures appropriate to many waveguide lasers, the transition linewidth becomes proportional to pressure rather than being Doppler broadened. Then the gain is independent of density and tube diameter. These discharge and laser similarity laws are summarized in Table IV, where relations (11a) and (12a) refer to a constant linewidth that is Doppler broadened, and relations (11b) and (12b) refer to linewidths that are pressure broadened. The results show that the waveguide or narrow-diameter lasers scale as power per unit length, and not as power per unit volume. This result occurs, because it is the former that controls gas temperature in waveguide lasers. The result also presages the importance of gas cooling in larger devices.

In many waveguide lasers (atomic and molecular) it is extremely difficult to obtain a stable dc discharge without additional RF excitation. As demonstrated long ago, two conditions must be satisfied to obtain a stable discharge: the ballast resistor (or its diode impedance equivalent) must be greater than the absolute value of the differential resistance R of the discharge, and the ballast also must be lower than (L/CR), where L is the inductance of the discharge and C is the capacitance between anode and cathode. Many discharges in capillaries or with limited cathode area have rapidly changing $V-I$ curves at low currents, and it is difficult to run a stable discharge. Such circumstances led to adoption of RF excitation.

TABLE IV
SIMILARITY RELATIONS FOR MOLECULAR LASER AND ATOMIC LASER DISCHARGES. (AFTER KONYUKHOV, [74]). THE TABLE INDICATES THE DISCHARGE RESPONSE TO CHANGES IN TUBE RADIUS AND GAS PRESSURE THAT KEEP PR CONSTANT.

Parameters	Molecular Laser Discharge	Atomic Laser Discharge (low-current density)
(1) Dimensions	$R_1/R_2=a$	Assume $L_1=L_2a$, $R_1=R_2a$
(2) Gas temperature	$Tg_2=Tg_1$	Assume $V_2=V_1$; Tg=constant
(3) Electron temperature	$Te_2=Te_1$	$Te_2=Te_1$
(4) Gas pressure	$P_2=P_1a$	$P_2=P_1a$
(5) Gas number density	$N_2=N_1a$	$N_2=N_1a$
(6) Electron density	$Ne_2=Ne_1a$	$Ne_2=Ne_1a^2$
(7) Current density	$J_2=J_1a$	$J_2=J_1a^2$
(8) Current	$I_2=I_1/a$	$I_2=I_1$
(9) Electric field	$E_2=E_1a$	$E_2=E_1a$
(10) Power input/length	$P_2=P_1$	$P_2=P_1a$
(11a) Gain coefficient	$\varkappa_2=\varkappa_1a$	Higher current laser discharges involve "forbidden" similarity processes such as step excitation and ionization, and recombination
(11b) —	$\varkappa_2=\varkappa_1$	
(12a) Saturation flux density	$S_2=S_1a$	
(12b) —	$P_2=P_1a^2$	
(13) Power out/volume	$PL_2=PL_1$	

The Schottky diffusion theory of the positive column, although often quoted with respect to molecular gas lasers, does not apply. The Schottky model predicts a discharge voltage that is independent of current. While nonlinear terms in ionization or loss will give a falling characteristic D, Schuocker *et al.* [75] showed that for narrow-bore helium–neon discharges these effects are insufficient to describe the experimental observations. The inclusion of a wall sheath of reasonable extension was shown to model the observed results. The sheath thickness increases with electron temperature and with decreasing charge density. Therefore the effects of the finite wall sheath are more important at lower discharge currents when the discharge plasma volume is actually constricted by the sheath extension. These conclusions, while originally derived for rare gas lasers, also apply to molecular gases.

For low-pressure larger radius discharges, the principal cooling is by thermal diffusion to the boundaries; that is,

$$div(k\ grad\ T) + Q = 0. \tag{16}$$

The profile of the heating term Q is controlled by the electron density profile. To first order, the Bessel function may be approximated by a parabolic function $Q = Q_o[1 - (r^2/R^2)]$, where Q_o is the on-axis value. The temperature difference between the discharge axis and tube wall is then given by

$$\Delta T = \frac{3EI(1-\eta)}{8pk_{\text{mix}}} \tag{17}$$

where k_{mix} is the species-averaged thermal conductivity, E is the discharge electric field, I is the discharge current, and η is the laser efficiency. The difference in gas temperature is independent of tube radius. For a CO_2:N_2:He, 1:2:3 mixture,

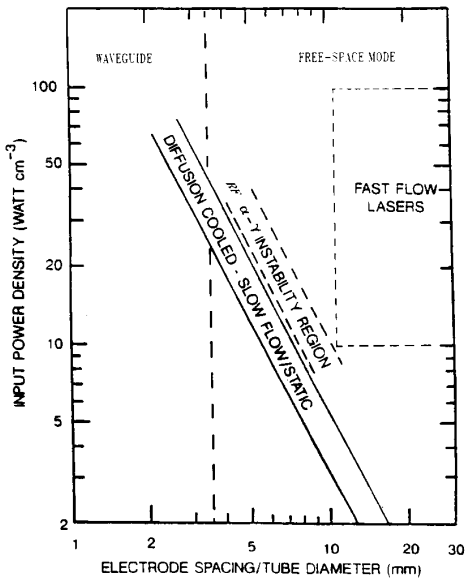

Fig. 11. Electrical input power density in diffusion-cooled and fast-flow lasers. The power density for alpha-to-gamma discharge-mode transition is shown for diffusion-cooled lasers at the optimum excitation frequency (after [76]). One wishes to operate at high frequencies in the alpha-mode at power densities below the transition line to maintain efficient and uniform excitation.

$k \sim 10^{-3}$W/cm/K. The maximum temperature difference tolerable ($\sim$ 300 K) translates to a maximum laser output of 50 W/m at an efficiency of 20%. Several methods have been used to overcome this temperature limitation. Hall *et al.* [76] have readdressed the waveguide laser and pointed out the importance of area scaling. For higher power lasers this limitation is overcome by high velocity flow to provide heat rejection (see below).

If one considers a uniform discharge between a cooled metal plate of width w, length L, and spacing d, then the total laser power extractable from the volume is $P_l = fP_s(w/d)L$, where f is a geometric factor allowing for two-wall cooling, and PL is the specific power for a square cross-section gain medium (defined by Hall *et al.* as approximately 80 W/m). Consequently, the power of a waveguide laser should scale as$P = f(PL/d)A$. Subject to the requirement of no decrease in energy deposition efficiency, this suggests that for a chosen d the lasers will scale with electrode area A. Experiments validating these ideas have recently been reported [76]. A 376-mm-long CO_2 discharge excited at 125 MHz gave power extraction scaling as 20 kW/m^2 in the one-dimensional cooling regime. The scaling of the input power density versus the electrode spacing (for waveguides) or versus the tube diameter for a free-space cavity mode laser is illustrated in Fig. 11. Fast flow lasers are really only economical for higher power lasers and so have been given a power density threshold.

The importance of efficient coupling of RF energy to the laser discharges must be emphasized. RF matching networks are used in RF plasma reactors, and a similar but distributed matching is required for the RF-excited lasers. It is necessary that the matching condition be at least approximated, such that the impedance of the load as seen by the RF source is the complex conjugate of the impedance of the generator as seen by the load. An analysis relevant to waveguide lasers has been provided by Moghbeli *et al.* [77], and while it was derived with CO_2 waveguide lasers in mind, it has reasonably generic applicability. There are two similar principal RF excitation approaches. The first uses metal electrodes sandwiched between ceramic pieces to provide a hollow waveguide. It is found that more efficient operation is obtained when the excitation frequency is high where the sheath fields are lower. However, at higher frequencies and longer waveguide lengths the RF wavelength is comparable to the discharge length, and nonuniform fields cause nonuniform discharges. This effect is overcome by using distributed shunt inductors. The inductors provide a negative admittance to compensate for the variation in phase angle of the transmission-line reflection coefficient along the length of the laser. The inductors are of equal value except the end inductors, which have twice the value of the others. The second approach is the parallel-resonant distributed inductance developed by Newman *et al.* [78]. The ceramic pieces are sandwiched between the electrodes to form a relatively high capacitance structure. Many discrete inductances are used to approximate uniformly distributed inductances. The magnitude of the inductance is adjusted to provide an LC resonance at the excitation frequency. This second method is becoming more important, because it permits power scaling by increasing the area of the electrode or by use of coupled discharges to give phased-array structures.

D. High-Energy Lasers

Scaling to power levels of more than a few hundred watts requires convective cooling of the laser. The mass flow required $\dot{m}$, to limit the temperature rise to ΔT K, is given by

$$\dot{m} = \frac{P(1-\eta)}{c_p \Delta T}. \tag{18}$$

The CO_2 1:2:3 mixture corresponds to an equivalent 18.7 gm/mol and a specific heat, c_p = 26 J/mol/K. The gas density is 8.4×10^{-4}gm/cm^3. These figures translate into $\dot{m} = 0.025$ lb/s/kW. For powers greater than a kilowatt, this flow is difficult to achieve at low pressures and so gives an incentive to consider pressure scaling. While the CO_2 laser again will be considered, the concepts apply to other molecular gas systems.

The input power is given by $P = jE = qn_e wE$, where w is the electron drift velocity. To achieve high efficiency, an (E/N) is selected and the fractional ionization is kept constant. Therefore $P = q(nE/N).W.N^2$ or $P \propto N^2$ if the conditions are met. At low pressures, E/N must be high enough to provide an ionization frequency that balances the losses due to diffusion, recombination, and attachment. At high pressures the ionization can be provided by electron beams, which then permit tuning of the E/N of the pumping discharge to obtain maximum efficiency. This approach benefited from the energy-deposit ion studies performed many years earlier by Berger and Seltzer [79]. Pumping efficiency curves have been provided by various authors [80].

Eventually, the CO_2 electrical laser becomes a victim of its high efficiency. This occurs when the relaxation of the lower

laser level is fast enough and provides sufficient energy to modify the flowing-gas properties. The effect has been named "mode-medium interaction."

The RF discharge was investigated by Levitskii [81], who classified two principal modes: a so-called alpha discharge at low-current discharges with distinct electrode sheaths and volume (Townsend) ionization; and a second, gamma-mode, at higher current densities where the discharge is maintained by secondary electron emission caused by ion bombardment of the electrodes. (A contemporary approach [82] would introduce the influences of excitation frequency, collisionless energy transfer, and wave-riding.) These excitation mechanisms can cause spatial discharge inhomogeneities. Optimum excitation frequencies which vary inversely with the electrode spacing are found to be typically 120 MHz at $d = 2.75$ mm. Too low a frequency gives the γ-mode, whose fast electrons cause excessive dissociation for CO_2-based lasers and probably most other molecular infrared lasers as well. The transfer of the models and analyses developed for RF processing discharges to RF-excited lasers has not been made. However, empirical advances in coupling several waveguide lasers by means of ridge coupled areas, driven by one RF source, point the way to new discharge configurations suitable for phased-array operation.

Scaling to high pressures was also achieved by pulsed high-pressure discharges. These relate to the early work on impulse breakdown studies by the school of Meek and Craggs [83]. To avoid extremely high voltages, Dumanchin and Rocca-Serra [84] first excited high-pressure (420 torr) CO_2 in transverse geometry. Beaulieu [85] used 17-kV short-10's of ns pulses to excite an atmospheric pressure discharge where the distributed excitation was achieved by using a row of sharp pins as a cathode. Many configurations and preionization schemes have been investigated, including X-rays, double pulses, photoionization, and auxiliary discharges. Lin and Levalter [86] defined the preionization conditions necessary to achieve uniformity of the laser discharge. The technology has been reviewed by Wood [87], and more recently by Brown [88].

E. Discharge Chemistry

The detailed analysis of infrared lasers has invoked many aspects of discharge physics. Calculations of the electron-energy distribution functions by solving the Boltzmann transport equation were assisted by the methods established much earlier by discharge research and electron transport research. These calculations were made for given input cross sections, E/N values, and an assumed gas mixture. Rapid progress was possible since the codes were essentially established by early work, especially that of Frost and Phelps [89]. These calculations were not self-consistent, in that they did not consider dissociation or the resultant chemistry. Furthermore, the traditional drift experiments studiously had avoided such real-life problems. Nighan *et al.* [90] were among the first to show that the influences of plasma-induced chemistry and negative ions were very important for long-life, sealed-off operation and for higher energy-density discharge stability. To analyze these phenomena, the quantitative databases on electron attachment and dissociation were invaluable. There are several methods to overcome the adverse effects of dissociation of CO_2 on laser operation. In sealed systems it is possible to provide the required ionization level with reduced dissociation levels by adding a small percentage of xenon to the traditional gas mixture. The use of xenon is attractive, since it does not react chemically with the other species and has a large ionization cross section and a low ionization potential. In principle, one could use metal additives, but these lead to difficulties with control of the vapor pressure and condensation on optical components. Alternatively, CO or H_2 may be added to the mixture to enhance detachment of negative ions. A third method to reduce the dissociation of CO_2 is to include heterogeneous catalysts in the system. Materials that have been used include hopcalite, platinum, and gold [91]. Browne and Smith [92] demonstrated that while a platinum catalyst in a low-pressure CW CO_2–N_2–He–Xe laser resulted in a long lifetime, the further addition of hydrogen or deuterium was deleterious. In other words, the benefits of reassociation had already been obtained and the hydrogen then only decreased the population of the upper laser level.

In flowing lasers and at high pressures it is not economical to use xenon, and then one does use additives such as H_2O, O_2, and H_2. Shields *et al.* [93] constructed a comprehensive kinetic model of negative ion formation in such discharges and also compared the low-pressure results of Prince and Garscadden [94]. At high pressures, CO_3^- is the dominant negative ion, while at low pressure the negative ions of the oxides of nitrogen and the oxygen negative ions are more important. An analysis by Hokazono and Fujimoto [95] used 175 kinetic equations for the plasma chemistry in a TEA laser and obtained a useful engineering rule that the fractional decomposition was almost proportional to the energy deposited/pulse. Calculations of the effects of additive CO, H_2, and H_2O showed the last to be most effective in reforming CO_2; however, this criterion alone is not sufficient, since no account is made of the effects of the additives on the plasma stability.

F. Discharge Instabilities

The problem of arcing at high pressures is an old one. Several authors [96]–[98] have suggested that the presence of a sufficient density of negative ions enhances arcing in TEA lasers based on CO_2 and other gases or gas mixtures. At high-energy loading the actual arcing often appears to be a combination of an ionization and a thermal instability. The ionization instability in an infrared molecular gas mixture is, strictly speaking, an attachment-ionization-recombination instability. It occurs in both self-contained and externally sustained charges. These instabilities have properties similar to the classical moving striations [97]. Temporal-spatial inhomogeneities adversely affect the quality of the laser medium and sometimes provide a trigger mechanism for the onset of constriction and arcing. Thus the uncontrolled plasma chemistry can lead to degraded long-term performance of low-power lasers and catastrophic failure of high-power lasers. The degradation can occur also due to vibrational quenching by the impurities, and, more seriously, to the dissociation of the lasing species.

The attachment instability requires an electron-attachment rate which increases rapidly with electron temperature. The necessary condition was expressed by Nighan and Wiegand [97] as

$$\frac{k_a \hat{k}_a}{k_i \hat{k}_i} > 1 \tag{19}$$

where k_a and k_i are the attachment and ionization rates, and the caret notation denotes their logarithmic derivatives with respect to T_e. The mechanism of the instability can be described heuristically as being similar to a striation. Neglecting the phase relations, an increase in electron temperature will cause an increase in negative ion density, and a decrease in the local electron density. There is therefore a decrease in the local plasma conductivity. If the circuit conditions require a constant current, the local electric field will increase, which further increases the attachment rate and thus leads to instability. The sufficient conditions for instability involve the electron–ion and ion–ion recombination rates and most importantly, the detachment rate k_d. As the current density in the discharge increases, k_d must be made larger to ensure stability. The amplitude cycle of the instability can be established by numerically solving the continuity equations for the three charged species. Examples of such calculations are give by Long *et al.* [99] for a CO_2:N_2:He laser mix and the effects of O_2 and CO. These results were confirmed by Beverly [100]. In principle, the influences of the discharge modulations on the laser output can be calculated. The neutral plasma chemistry occurs on a longer time scale (Table II) and hence can be calculated separately to establish the neutral densities. The negative ion-chemistry calculations by Shields *et al.* [93] showed that small amounts of oxygen were especially troublesome to the uniformity of atmospheric TEA CO_2 lasers. The preionization electrons are lost rapidly to molecular oxygen by three-body attachment. This effect greatly reduces the permissible time window between the preionization pulse and main discharge. Thus the collisional processes and plasma chemistry actually determine the requirements and sophistication of the circuit hardware needed for reproducible and efficient lasing.

The interest in high-pressure lasers led gas discharge research into parameter regimes that were entirely new. The e-beam-sustained discharge may satisfy the quoted conditions for stability; however, the discharges will often still form arcs. The theory previously referenced is for a homogeneous unbounded plasma; there is no account of the phenomena at the boundaries. Arc formation in such e-beam-sustained plasmas was studied by Douglas-Hamilton [101]. A major finding was the identification and measurement of discharge streamers (usually but not always initiated at the cathode) which propagate into the discharge and often lead to shorting of the gap. The streamer growth rate was determined to be exponential. Based on the framing camera measurements and shadowgraphs, a model was devised wherein the streamer is represented as a quasi-thermal arc concentrating the current flow and enhancing the electric field at its leading tip. The initiation of the streamer at the cathode is caused by a local inhomogeneity in cathode emission, which in turn results in the local heating and expansion of the cathode gas layer against the more dense background gas. A possible explanation is that there is a coupling of the fluid-dynamic Rayleigh–Taylor instability with the ionization and thermal instabilities of the plasma.

The carbon monoxide laser is one in which all of the degrees of freedom of the molecule play important roles in the laser mechanism and efficiency. The laser depends on the vibrational excitation by anharmonic pumping through vibrational–vibrational (V-V) energy transfer. Carbon monoxide is slightly anharmonic and the energy spacing between vibrational levels becomes smaller with an increase in the vibrational level. The energy is redistributed by the process:

$$\mathrm{CO}(v) + \mathrm{CO}(v') \rightarrow \mathrm{CO}(v+1) + \mathrm{CO}(v'-1) \tag{20}$$

where $v' < v$. The forward process is strongly favored at low translational–rotational temperature. The CO(v) is excited by electron collisions up to approximately v=7. The higher vibrational levels are then populated in a non-Boltzmann distribution by anharmonic pumping. In carbon monoxide at lower v's, the V–V energy transfer rates are orders of magnitude faster than the vibrational–translational (V–T) energy-transfer rates. Trainor *et al.* [102] showed that when there is strong excitation of the lower vibrational levels and decoupling of the vibrational manifold from the translational mode, the upper levels of the vibrational manifold are overpopulated with respect to the equivalent Boltzmann distribution for the same vibrational energy content. Due to their higher small signal gains, almost all CO lasers operate on the P transitions from vibrational rotational states (V, J)→(V-1, J+1), which permit lasing on partial inversions. The lasing occurs in cascading transitions, because when one transition reaches threshold, it depletes the lower level of the transition above it and populates the upper level of the transition below it. These effects lead to operation on a series of transitions and a high quantum efficiency. Overall efficiencies of higher than 60% have been reported [103]. The high output coupling possible with CO produces very obvious optogalvanic effects which illustrate the need for inclusion of collisions of the second kind in modeling this laser. Prior to the CO laser there had been few studies on cryogenically cooled discharges. The requirement of low translational temperatures led to a revival of interest in discharges with cryogenic wall cooling or in supersonic expanding flows. Reilly [104] identifies the latter as a class where the discharge has volumetric temperature control. In this case, there is a one-dimensional power balance of flow heating versus the discharge power input:

$$rUc_p \frac{dT_g}{dz} = J.E. = \frac{e^2}{m_e} n_e N \left(\frac{E}{N}\right)^2 (\bar{\sigma}_m, v_e) \tag{21}$$

where r and c_p are the gas density and specific heat, respectively, U is the gas velocity, dT_g/dz is the rate of temperature increase with distance, and v_e is the electron thermal speed. The important point is that as the gas density increases while the power input increases at a fixed (E/N),

the capability of the gas to absorb the power also increases with gas density.

Shapiro [105] has analyzed the situation of heat input to gas flow in a channel of constant-area cross section and showed that both subsonic and supersonic flows will tend to Mach number = 1. Rayleigh line calculations for energy input approximately equal to the translational flow energy show that inlet Mach numbers must be less than 0.15 to avoid density changes greater than a factor of two. Choking will occur for inlet Mach numbers of $\sim$ 0.4 [104]. Thus in CW and repetitively pulsed devices the average power is limited by the maximum flow velocity; in short-pulse (less than the flow transit time) devices the pulse energy is limited by the maximum gas temperature permissible.

Gas purity is very important in the carbon monoxide systems, since it is necessary to avoid any species that quench the vibrational manifold. The anharmonicity of CO means that there is usually a resonance energy transfer to the impurity from some levels of the CO. Some species such as the pentacarbonyls cause extremely fast V–T rates.

As one moves into the submillimeter region the discharges required become longer and larger in cross section. These oscillators have been used as reference frequencies and for plasma interferometry. The difficulties, such as toxicity, of working with HCN, CS_2, etc., have restricted their uses thus far. (There are also considerable problems with sealed-off operation that have received little attention.) As an interesting example of such discharges, Pollack *et al.* [106] ran a 1-A water-cooled discharge, 3 m in length with a 7.5-cm ID. The water vapor laser displayed at least 65 pulsed lines, ranging from 47 to 79 μm and 9 CW lines.

The extension of discharge excitation techniques to far-infrared transitions that involve pure rotational transitions becomes one of limiting returns. The quantum efficiency becomes the ratio of the rotational quantum to at least one vibrational quantum. The discharge excitation also introduces the problems of plasma chemistry and gas cooling. Therefore it is much easier, if appropriate laser pumping sources exist, to use optical excitation of the far-infrared transition. The overall efficiencies are about the same since, in either case, one is still using a discharge to provide the vibrational laser.

Discharge lasers that are electrical–chemical in nature can accommodate more intense and higher E/N discharges. Such methods include microwave excitation [107], [108] or e-beam stabilized discharges [109]. In these systems there are probably contributions to population inversion from recombination reactions into excited products.

G. Future Prospects

Initially, much of the research tended to concentrate on the scaling of infrared lasers; however, more recently there has been a new emphasis on long lifetime and reliability. This trend is expected to continue and expand from the CO_2 and CO systems to other infrared lasers. Improvements do not come easily, since a large database is required to model and design such lasers. The modeling requires information on a large number of processes: (a) electron-impact excitation and ionization; (b) ion impact, especially dissociative charge transfer in polyatomic species; (c) V–T relaxation rates; (d) V–V–T near resonance exchange collisions; (e) spontaneous decay rates, including $\Delta v = 1$ and $\Delta v = 2$; (f) stimulated emission cross sections and line-broadening parameters; and (g) miscellaneous processes involved in the conditions related to discharge uniformity and stability such as UV ionization processes, attachment, and detachment rates. Research into collisional processes has benefited the CO laser—some of the recent impressive gains in the CO-laser performance and applications are reviewed by Maisenhalder [110]. Similar improvements are considered possible for other laboratory infrared lasers.

It is anticipated that more practical designs for high-pressure operation of gas discharges will evolve due to the interest in tunable lasers and in very short pulse lasers. The necessary operating pressure for continuous frequency tuning is about 5 atm for a mixture of CO_2 isotopes, and 10 atm for a single isotope [111]. There are many applications in spectroscopy, short-pulse phenomena, ranging, optical pumping, and relaxation processes to encourage this development. It appears that distributed (meander-line or slow-wave applicator) microwave excitation may play a role in discharge excitation, in addition to the waveguide devices utilized so far.

Gas-phase approaches to the near-millimeter wave-source problem have been reviewed by De Lucia *et al.* [112]. The gas-phase approach is still attractive for higher power devices. It should be possible to revisit these devices with a better understanding of the plasma conditions required for laser operation. Also, new excitation techniques and configurations offer enhanced performance. Several of the ideas used in plasma processing, such as extended multipole plasma confinement and electron-cyclotron resonance plasmas, appear attractive and may serve to change such lasers from laboratory devices to established sources. Electrical–chemical lasers operating in the infrared, similar to those discussed in Section III, are anticipated. Materials and catalyst developments may not only regenerate the lasing species, but also deliver vibrationally excited molecules [113], [114].

Other configurations of great interest will be those that are modular [78], [115] and compatible with phased-array operation. Hart *et al.* [115] have demonstrated mode locking and efficiency in CO_2 using a staggered waveguide approach (68 W in a 6-element array). The machining techniques and optical gratings for longer wavelength operation should be easier and less expensive than those required below 12 μm. Some remarkable claims of a very large number (61) of coupled discharge lasers have been made [116] at 10.6 μm.

ACKNOWLEDGMENT

The authors thank their colleagues for comments and references, especially E. A. McLean for suggestions regarding the short-wavelength laser portion of the text.

REFERENCES

[1] R. C. Tolman, "Duration of molecules in upper quantum states," *Phys. Rev.*, vol. 23, pp. 693–709, 1924.

[2] R. Ladenburg, "Dispersion in electrically excited gases," *Rev. Mod. Phys.*, vol. 5, pp. 243–256, 1933 (and references therein).

[3] V. A. Fabrikant, "The emission mechanism of gas discharges," *Trans. Electrotekhn. Inst.*, vol. 41, p. 254, 1940 (quoted in C. G. B. Garrett, *Gas Lasers*. New York: McGraw-Hill, 1967, chap. 1).

[4] B. A. Lengyel, *Introduction to Laser Physics*. New York: Wiley, 1966, p. 184.

[5] R. W. Waynant and R. C. Elton, "Review of short wavelength laser research," *Proc. IEEE*, vol. 64, pp. 1059–1092, July, 1976.

[6] D. L. Matthews *et al.*, "Demonstration of a soft-X-ray amplifier," *Phys. Rev. Lett.*, vol. 54, p. 110, 1985.

[7] *Proc. Opt. Soc. Amer. on Shortwavelength Coherent Radiation: Generation and Applications*, R. W. Falcone and J. Kirz, Eds. Washington, DC: Opt. Soc. Amer., 1988.

[8] B. J. MacGowan *et al.*, "Progress toward a 44 Å X-ray laser," in *Proc. Opt. Soc. Amer. on Shortwavelength Coherent Radiation: Generation and Applications*, R. W. Falcone and J. Kirz, Eds. Washington, DC: Opt. Soc. Amer., 1988, pp. 2–10.

[9] M. D. Rosen *et al.*, "Exploding-foil technique for achieving a soft X-ray laser," *Phys. Rev. Lett.*, vol. 54, pp. 106–109, Jan. 1985.

[10] T. N. Lee, E. A. McLean, and R. C. Elton, "Soft X-ray lasing in neonlike germanium and copper," *Phys. Rev. Lett.*, vol. 59, pp. 1185–1188, Sept. 1987.

[11] T. N. Lee, E. A. McLean, J. A. Stamper, H. R. Griem, and C. K. Manka, "Laser-driven soft X-ray experiments at NRL," *Bull. Amer. Phys. Soc.*, vol. 33, p. 1920, 1988.

[12] M. D. Rosen, R. A. London, and P. L. Hagelstein, "The scaling of Ne-like X-ray laser schemes to short wavelength," *Phys. Fluids*, vol. 31, pp. 666–670, 1988.

[13] R. C. Elton, *X-Ray Lasers*. New York: Academic, 1990.

[14] S. Suckewer, C. H. Skinner, H. Milchberg, C. Keane, and D. Voorhees, "Amplification of stimulated soft X-ray emission in a confined plasma column," *Phys. Rev. Lett.*, vol. 55, pp. 1753–1756, Oct. 1985.

[15] S. Suckewer *et al.*, "Divergence measurements of soft X-ray laser beam," *Phys. Rev. Lett.*, vol. 57, pp. 1004–1007, Aug. 1986.

[16] P. L. Hagelstein, "Short wavelength lasers: something new, something old," in *Proc. Opt. Soc. Amer. on Shortwavelength Coherent Radiation: Generation and Applications*, R. W. Falcone and J. Kirz, Eds. Washington, DC: Opt. Soc. Amer., 1988, pp. 28–35.

[17] S. Suckewer, "X-ray related experiments and theory at Princeton," in *Proc. Opt. Soc. Amer. on Shortwavelength Coherent Radiation: Generation and Applications*, R. W. Falcone and J. Kirz, Eds. Washington, DC: Opt. Soc. Amer., 1988, pp. 36–46.

[18] H. C. Kapteyn, R. W. Lee, and R. W. Falcone, "Observation of a short wavelength laser pumped by Auger decay," *Phys. Rev. Lett.*, vol. 57, pp. 2939–2942, Dec. 1986.

[19] W. T. Silfvast and O. R. Wood II, "Photoionization lasers pumped by broadband soft X-ray flux from laser-produced plasmas," *J. Opt. Soc. Amer. B*, vol. 4, pp. 609–618, Apr. 1987.

[20] M. H. Sher, J. J. Macklin, J. F. Young, and S. E. Harris, "Saturation of the Xe III 109 nm laser using traveling-wave laser-produced plasma excitation," *Opt. Lett.*, vol. 12, pp. 891–893, Nov. 1987.

[21] C. P. J. Barty *et al.*, "12.8 eV laser in neutral cesium," *Phys. Rev. Lett.*, vol. 61, pp. 2201–2204, Nov. 1988.

[22] J. J. Rocca, J. D. Meyer, and G. J. Collins, "1 W CW Zn ion laser," *Appl. Phys. Lett.*, vol. 43, pp. 37–39, 1983; see also, B. Wernsman *et al.*, "CW silver ion laser with electron beam excitation," *IEEE J. Quant. Electron.*, vol. QE-24, pp. 1554–1556, 1988.

[23] B. Wernsman, J. J. Rocca, and H. L. Mancini, "CW ultraviolet and visible laser action from ionized silver in an electron beam generated plasma," *IEEE Photon. Tech. Lett.*, vol. 2, pp. 12–14, Jan. 1990.

[24] J. J. Rocca, M. C. Marconi, M. Villagran Muniz, and D. C. Beethe, "Capillary discharge plasmas as extreme ultraviolet laser sources," in *Proc. Opt. Soc. Amer. on Shortwavelength Coherent Radiation: Generation and Applications*, R. W. Falcone and J. Kirz, Eds. Washington, DC: Opt. Soc. Amer., 1988, pp. 99–105.

[25] A. B. Petersen, "CW ion laser operation in argon, krypton and xenon at wavelengths down to 232 nm," in *Proc. Ann. Meet. IEEE Lasers and Electro-Optics Soc. (LEOS '89)* (Orlando FL), Oct. 1989; see also, "Short wavelength CW rare gas ion lasers," in *Proc. Eng. Found. Conf. on Future Prospects and Appl. for UV and VUV Lasers* (Santa Barbara, CA), Feb. 1990.

[26] K. Yamada, K. Miyazaki, T. Hasama, and T. Sato, "High power discharge-pumped F_2 molecular laser," *Appl. Phys. Lett.*, vol. 54, pp. 597–599, Feb. 1989.

[27] Y.-P. Kim, M. Obara, and T. Suzuki, "Theoretical evaluation of electron beam excited vacuum ultraviolet F_2 lasers," *J. Appl. Phys.*, vol. 59, pp. 1815–1818, Mar. 1986.

[28] M. Ohwa and M. Obara, "Theoretical evaluation of high efficiency operation of discharge-pumped vacuum ultraviolet F_2 lasers," *Appl. Phys. Lett.*, vol. 51, pp. 958–960, Sept. 1987.

[29] S. J. Benerofe, G.-Y. Yin, C. P. J. Party, J. F. Young, and S. E. Harris, "116 nm H_2," *Phys. Rev. Lett.*, vol. 66, pp. 3136–3139, June 1991.

[30] R. Sauerbrey and H. Langhoff, "Excimer ions as possible candidates for VUV and XUV lasers," *IEEE J. Quant. Electron.*, vol. QE-21, pp. 179–181, Mar. 1985.

[31] C. A. Brau, in *Excimer Lasers*," C. K. Rhodes, Eds. Berlin: Springer, 1979, pp. 87–134.

[32] R. S. Taylor and K. E. Leopold, "Ultralong optical-pulse corona preionized XeCl laser," *J. Appl. Phys.*, vol. 65, pp. 22–27, 1989.

[33] S. Watanabe and A. Endoh, "Wide aperture self-sustained discharge KrF and XeCl lasers," *Appl. Phys. Lett.*, vol. 41, pp. 799–801, 1982.

[34] G. J. Hirst, V. Rivano, and C. E. Webb, "Spatially resolved gain measurements in a discharge-pumped KrF laser amplifier," *J. Appl. Phys.*, vol. 61, pp. 2438–2444, 1987.

[35] C. H. Fisher *et al.*, "High efficiency XeCl laser excitation with magnetic switching," *Appl. Phys. Lett.*, vol. 48, pp. 1574–1576, 1986.

[36] W. H. Long, M. J. Plummer, and E. A. Stappaerts, "Efficient discharge pumping of an XeCl laser using a high-voltage prepulse," *Appl. Phys. Lett.*, vol. 43, pp. 735–737, 1983.

[37] R. S. Taylor and K. Leopold, "Microsecond duration optical pulses from a UV-preionized XeCl laser," *Appl. Phys. Lett.*, vol. 47, pp. 81–83, 1985.

[38] K. Midorikawa, M. Obara, and T. Fujioka, "X-ray preionization of rare gas–halide lasers," *IEEE J. Quant. Electron.*, vol. QE-20, pp. 198–205, 1984.

[39] M. R. Osborne, "Preionized electron density and ion decay measurements in an X-ray preionized rare gas fluoride laser," *J. Appl. Phys.*, vol. 63, pp. 32–37, 1988.

[40] T. S. Fahlen, "Efficient quarter-joule KrF laser with corona preionization," *IEEE J. Quant. Electron.*, vol. QE-15, pp. 311–313, 1979.

[41] P. Oesterlin and D. Bastling, "Eureka's excimers," *Phys. World*, vol. 3, pp. 43–46, 1990.

[42] T. Hasama, K. Miyazaki, K. Yamada, and T. Sato, "50 J discharge pumped XeCl laser," *IEEE J. Quant. Electron.*, vol. 25, pp. 113–120, 1989.

[43] L. F. Champagne, A. J. Dudas, and N. W. Harris, "Current rise-time limitations of the large volume X-ray preionized discharge-pumped XeCl laser," *J. Appl. Phys.*, vol. 62, pp. 1576–1584, 1987.

[44] W. L. Morgan, J. N. Bardsley, J. Kin, and B. L. Whitten, "Theory of ion–ion recombination in plasmas," *Phys. Rev.*, vol. A26, pp. 1696–1703, 1982.

[45] M. R. Flannery and T. P. Yang, "Three-body ion–ion recombination in mercury–halide lasers," *Chem. Phys. Lett.*, vol. 56, pp. 143–147, 1978.

[46] J. E. Velazco, J. H. Koltz, and D. W. Setser, "Quenching rate constants for metastable argon, krypton and xenon atoms by fluoride containing molecules, and branching ratios for XeF* and KrF* formation," *J. Chem. Phys.*, vol. 65, pp. 3468–3480, 1976.

[47] A. Kvaran, M. J. Shaw, and J. P. Simons, "Vibrational relaxation of KrF* and XeCl* by rare gases," *Appl. Phys. B*, vol. 46, pp. 95–102, 1988.

[48] W. J. Witteman and B. M. H. H. Kleikamp, "On the electron-beam pumped KrF laser," *J. Appl. Phys.*, vol. 55, pp. 1299–1307, 1984.

[49] M. Hayashi, "Recommended values of transport cross sections," Nagoya Instit. Tech., Rep. No. IPPJ-AM-19, 1981.

[50] R. E. Olsen, J. R. Peterson, and J. Moseley, "Ion–ion recombination total cross-sections atomic species," *J. Chem. Phys.*, vol. 53, pp. 3391–3397, 1970.

[51] R. S. Taylor, "Preionization and discharge stability study of long optical pulse duration UV-preionized XeCl lasers," *Appl. Phys. B*, vol. 41, pp. 1–44, 1986.

[52] S. Suminda *et al.*, "Effect of preionization uniformity on a KrF laser," *J. Appl. Phys.*, vol. 52, pp. 2682–2686, 1981.

[53] S. Watanabe, A. J. Alcock, K. E. Leopold, and R. S. Taylor, "Spatially resolved gain measurements in UV preionized homogeneous discharge XeCl and KrF lasers," *Appl. Phys. Lett.*, vol. 38, pp. 3–6, 1981.

[54] A. B. Treshchalov and V. E. Peet, "Spatial-time dynamics of the discharge pumping and lasing in a XeCl excimer laser," *IEEE J. Quant. Electron.*, vol. 24, pp. 169–176, 1988.

[55] M. J. Kushner and A. L. Pindroh, "Discharge constriction, photodetachment, and ionization instabilities in E-beam sustained discharge excimer lasers," *J. Appl. Phys.*, vol. 60, pp. 904–914, 1986.

[56] M. J. Kushner, A. L. Pindroh, C. H. Fisher, T. A. Znotins, and J. J. Ewing, "Multidimensional modeling of transverse avalanche laser

discharges," *J. Appl. Phys.*, vol. 57, pp. 2406–2423, 1985.
[57] M. J. Kushner, "Discharge instabilities initiated by nonuniform laser extraction in E-Beam sustained discharge KrF lasers," *J. Appl. Phys.*, vol. 62, pp. 101–107, 1987.
[58] *Handbook of Molecular Lasers*, P. K. Cheo, Ed. New York: Marcel Dekker, 1987.
[59] R. E. Center, "High-power, efficient electrically-excited CO lasers," in *Laser Handbook*, vol. 3, M. L. Stitch, Ed. Amsterdam: North-Holland, 1979.
[60] J. D. Daugherty, "Electron-beam ionized lasers," in *Principles of Laser Plasmas*, G. Bekefi, Ed. New York: Wiley, 1976.
[61] K. G. Emeleus and G. A. Woolsey, *Discharges in Electronegative Gases*. New York: Barnes and Noble, 1970.
[62] C. Kenty, "Dissociative recombination and the constriction of the positive column," in *Ionization Phenomena in Gases*, vol. 1, H. Maecker, Ed. Amsterdam: North-Holland, 1962, pp. 356–366.
[63] L. J. Kieffer, "A compilation of electron collision cross section data for modeling gas discharge lasers," *Joint Instit. Lab. Astrophys.*, Boulder, CO, Rep. No. 13, 1973 (revised 1978).
[64] J. S. E. Townsend, *Electrons in Gases*. London: Hutchinsons, 1947.
[65] G. J. Schulz, "Vibrational excitation of N_2, CO and H_2 by electron impact," *Phys. Rev. A*, vol. 135A, pp. 988–995, 1964.
[66] M.A. Pollack, "Molecular gas lasers," in *Handbook of Lasers*, R. J. Pressley, Ed. Cleveland, OH: CRC Press, 1971, pp. 298–349.
[67] J. C. Polanyi, "Proposal for an IR maser dependent on vibrational excitation," *J. Chem. Phys.*, vol. 34, pp. 347–349, 1961.
[68] L. E. S. Mathias and J. T. Parker, "Stimulated emission in the band spectrum of nitrogen," *Appl. Phys. Lett.*, vol. 3, pp. 16–18, 1963.
[69] "Energy transfer in gases," in Proc. 12th Chem. Conf., R. Stoops, Ed. New York: Interscience, 1963.
[70] C. K. N. Patel, "Continuous-wave laser action on vibrational-rotational transitions of CO_2," *Phys. Rev. Lett.*, vol. 336A, pp. 1187–1193, 1964.
[71] A. von Engel and M. Steenbeck, *Elektrische Gasetladungen* (Ihre Physik und Technik, I, II). Berlin: Springer-Verlag, 1934.
[72] G. Francis, "The glow discharge at low pressure," in *Encyclopedia of Physics*, vol. 22. Berlin: Springer-Verlag, 1956.
[73] R. L. Abrams, "Waveguide gas lasers," in *Laser Handbook*, vol. 3, M. L. Stitch, Ed. Amsterdam: North-Holland, 1979.
[74] V. K. Konyukhov, "Similar gas discharges for CO_2 lasers," *Soviet Phys.–Tech. Phys.*, vol. 15, pp. 1283–1287, 1971.
[75] D. Schuocker, W. Reif, and R. Erlacher, "Properties and current-voltage characteristics of discharges in waveguide gas lasers," *Appl. Phys.*, vol. 14, pp. 277–282, 1977.
[76] D. R. Hall and H. J. Baker, "RF excitation of diffusion cooled and fast axial flow lasers," in *Proc. 7th Int. Symp. on Gas Flow and Chemical Lasers*, SPIE, vol. 1031, pp. 60–67, 1988.
[77] F. Moghbeli, D. He, G. Allcock, and D. R. Hall, "Impedance matching in radio-frequency discharge excited waveguide lasers," *J. Phys. E*, vol. 17, pp. 1159–1164, 1984.
[78] L. A. Newman and R. A. Hart, "Recent advances in sealed-off CO_2 lasers," *Laser Focus*, vol. 23, pp. 80–86, 1987.
[79] J. J. Berger and S. M. Seltzer, Nat. Acad. Sci., Washington, DC, NAS-NRC 113 (Nucl. Sci. Series Rep. No. 10).
[80] D. H. Douglas Hamilton and R. S. Lowder, "Carbon dioxide electric discharge laser kinetics handbook," Avco Everett Res. Lab., Apr. 1975; see also, C. J. Elliott, O. P. Judd, A. M. Lockett, and S. D. Rockwood, "Electron transport coefficients and vibrational excitation rates for electrically excited CO_2 gas lasers," Los Alamos Nat. Lab., Los Alamos, NM, Rep.-5562-MS, 1974.
[81] S. M. Levitskii, "An investigation of the breakdown potential of a high-frequency plasma in the frequency and pressure transition regions," *Sov. Phys.–Tech. Phys.*, vol. 2, pp. 887–891, 1958.
[82] J. P. Bouef and P. Belenguer, in *Non-Equilibrium Processes in Partially Ionized Gases*, M. Capitelli and J. N. Bardsley, Eds. New York: Plenum, 1990.
[83] J. M. Meek and J. D. Craggs, *Electrical Breakdown of Gases*. New York: Wiley, 1978.
[84] R. Dumanchin and J. Rocca-Serra, "Augmentation de l'energie et de la puissance fournie par unite de volume dans un laser a CO_2 en regime pulse," *C. R. Acad. Sci.*, vol. 269, pp. 916–919, 1969.
[85] A. J. Beaulieu, "Transversely excited atmospheric pressure CO_2 laser," *Appl. Phys. Lett.*, vol. 16, pp. 504–506, 1970.
[86] S. C. Lin and J. I. Levatter, "X-ray preionization for electric discharge lasers," *Appl. Phys. Lett.*, vol. 34, pp. 505–508, 1979.
[87] O. R. Wood, "High-pressure molecular lasers," *Proc. IEEE*, vol. 62, pp. 355–397, 1974.
[88] R. T. Brown, "CO_2 TEA Lasers" in *Handbook of Molecular Lasers*, P. K. Cheo, Ed. New York: Marcel Dekker, 1987.
[89] L. S. Frost and A. V. Phelps, "Momentum transfer cross sections for slow electrons in He, Ar, Kr, and Xe using transport coefficients," *Phys. Rev.*, vol. 127, pp. 1621–1626, 1962; see also, *Phys. Rev.*, vol. 136, pp. 1538–1546, 1964.
[90] W. J. Wiegand and W. L. Nighan, "Plasma chemistry of CO_2–N_2–He discharges," *Appl. Phys. Lett.*, vol. 11, pp. 583–586, 1973.
[91] J. A. Macken, S. K. Yagnik, and M. A. Samis, "CO_2 laser performance with a distributed gold catalyst," *IEEE J. Quant. Electron.*, vol. 25, pp. 1695–1703, 1989.
[92] P. G. Browne and A. L. S. Smith, "Long-lived CO_2 lasers with distributed heterogeneous catalysis," *J. Phys. D: Appl. Phys.*, vol. 7, pp. 2464–2470, 1974.
[93] H. Shields, A. L. S. Smith, and B. Norris, "Negative ion effects in TEA CO_2 Lasers," *J. Phys. D: Appl. Phys.*, vol. 9, pp. 1587–1603, 1976.
[94] J. F. Prince and A. Garscadden, "Negative ion species in CO_2–N_2–He discharges," *Appl. Phys. Lett.*, vol. 27, pp. 13–15, 1975.
[95] H. Hokazono and H. Fujimoto, "Theoretical analysis of the CO_2 molecule decomposition and contaminants yield in transversely excited atmospheric CO_2 laser discharge," *J. Appl. Phys.*, vol. 62, pp. 1585–1594, 1987.
[96] D. H. Douglas-Hamilton and S. A. Mani, "An electron-attachment plasma instability," *Appl. Phys. Lett.*, vol. 23, pp. 508–510, 1973.
[97] W. L. Nighan, in *Principles of Laser Plasmas*, G. Bekefi, Ed. New York: Wiley, 1976; see also, W. L. Nighan and W. J. Wiegand, "Influence of negative-ion processes on steady-state properties and striations in molecular gas discharges," *Phys. Rev. A*, vol. A10, pp. 922–945, 1974.
[98] A. S. Kovalev, I. G. Peersiantsev, V. D. Pis'mennyi, and A. T. Raakhimov, "Instabilities of high-pressure glow discharges," in *Molecular Gas Lasers*, E. P. Velikov, Ed. Moscow: MIR, 1981, chap. 3.
[99] W. H. Long, W. F. Bailey, D. R. Pond, and A. Garscadden, presented at the IEEE 1st Int. Conf. on Plasma Sci., Knoxville, TN, 1974; published excerpts in W. J. Wiegand and W. L. Nighan, "Plasma chemistry of CO_2–N_2–He discharges," *Appl. Phys. Lett.*, vol. 11, pp. 583–586, 1973, and A. Garscadden, *Gaseous Electronics*, vol. I. New York: Academic, 1978, chap. 2.2.
[100] R. E. Beverly, "Ion aging effects on the dissociative-attachment instability in CO_2 lasers," *Opt. Quant. Electron.*, vol. 14, pp. 501–513, 1982.
[101] D. H. Douglas-Hamilton, "Investigation of the production of high density uniform plasmas," U.S. Air Force Wright Aeronautical Labs., Rep. 80–2087, AD No. A095508, 1980.
[102] C. E. Treanor, J. W. Rich, and R. G. Rehm, "Vibrational relaxation of anharmonic oscillators with exchange-dominated collisions," *J. Chem. Phys.*, vol. 48, p. 1728, 1968; see also, G. E. Caledonia and R. E. Center, "Vibrational distribution functions in anharmonic oscillators," *J. Chem. Phys.*, vol. 55, pp. 552–528, 1971.
[103] M. M. Mann, D. K. Rice, and R. G. Eguchi, "An experimental investigation of high energy CO lasers," *IEEE J. Quant. Electron.*, vol. QE-10, pp. 682–683, 1974.
[104] J. P. Reilly, "High-power electric discharge lasers," *Astronaut. Aeronaut.*, pp. 52–63, Mar. 1975.
[105] A. H. Shapiro, *The Dynamics and Thermodynamics of Compressible Flow*. New York: Ronald Press, 1953.
[106] M. A. Pollack, T. J. Bridges, and W. J. Tomlinson, "Competitive and cascade coupling between transitions in the CW water vapor laser," *Appl. Phys. Lett.*, vol. 10, pp. 253–255, 1967.
[107] D. S. Vasyutinskii, V. A. Kruzhalov, T. M. Perchanok, D. K. Terekin, and S. A. Fridrikhov, "Pulsed microwave discharge as a pump for the CO_2 laser," *Sov. Phys.–Tech. Phys.*, vol. 23, pp. 189–194, 1978.
[108] K. G. Handy and J. E. Brandelik, "Laser generation by pulsed 2.45 GHz microwave excitation," *J. Appl. Phys.*, vol. 49, pp. 3753–3756, 1978.
[109] S. R. Byron, L. Y. Nelson, and G. J. Mullaney, "HF and DF lasers by direct electrical discharge excitation," *Appl. Phys. Lett.*, vol. 23, pp. 565–567, 1973.
[110] F. Maisenhalder, "High power CO lasers and their application potential," in *Proc. 7th Int. Symp. on Gas Flow and Chem. Lasers, SPIE*, vol. 1031, pp. 98–111, 1988.
[111] S. Lovold and G. Wang, "Ten atmospheres high repetition rate RF-excited CO_2 waveguide laser," *Appl. Phys. Lett.*, vol. 40, pp. 13–15, 1982.
[112] F. C. DeLucia, E. Herbst, M. S. Field, and W. Happer, "Gas phase approaches to the near-millimeter wave source problem," *IEEE J. Quant. Electron.*, vol. QE-17, pp. 2171–2186, 1981.
[113] R. I. Hall, I. Cadez, M. Landau, F. Pichou, and C. Scherman, "Vibrational excitation of hydrogen via recombinative desorption of atomic hydrogen on a metal surface," *Phys. Rev. Lett.*, vol. 60, pp. 337–340, 1988.
[114] M. Kori and B. L. Halpern, "Vibrationally excited CO_2 from the reaction

of O atoms and adsorbed CO on platinum," *Chem. Phys. Lett.*, vol. 110, pp. 223–229, 1984.

[115] R. A. Hart, L. A. Newman, A. J. Cantor, and J. T. Kennedy, "Laser waveguide array," *Appl. Phys. Lett.*, vol. 51, pp. 1057–1059, 1987.

[116] A. F. Glova, Y. A. Dreizin, O. R. Kachurin, F. V. Lebedev, and V. D. Pis'mennyi, "Phase locking of a two-dimensional array of CO_2 waveguide lasers," *Sov. Tech. Phys. Lett.*, vol. 11, pp. 102–103, 1985.

Alan Garscadden (M'69–SM'71) was born in Scotland, and received the B.Sc. and Ph.D. degrees from Queen's University, Belfast, N. Ireland.

He emigrated to the U.S. and is now a Research Physicist at Wright–Patterson AFB (Ohio), where he studies collisional plasmas, electron transport, and laser diagnostics.

Dr. Garscadden is a Fellow of the American Physical Society.

Mark J. Kushner (S'74–M'79–SM'89–F'91) was born in Los Angeles, CA, in 1952. He received the B.A. degree in astronomy and the B.S. degree in engineering from the University of California, Los Angeles in 1976. He received the M.S. and Ph.D. degrees in applied physics from the California Institute of Technology, Pasadena, in 1977 and 1979, respectively, where he also held the position of Chaim Weizmann Postdoctoral Research Fellow.

He served on the technical staffs of the Sandia National Laboratory and Lawrence Livermore National Laboratory before joining Spectra Technology, Inc. (formerly Mathematical Sciences Northwest), where he was a Principal Research Scientist and Director of electron, atomic, and molecular physics. In August 1986 he joined the Department of Electrical and Computer Engineering at the University of Illinois (Urbana–Champaign), where he currently holds the rank of Associate Professor. He has published 70 refereed papers and presented more than 120 conference papers on topics related to gas and solid-state lasers, pulse power plasmas, plasma chemistry, chemical lasers, plasma processing of semiconductors, plasma treatment of toxic gases, and laser spectroscopy.

Dr. Kushner is a member of Phi Beta Kappa, Tau Beta Pi, Sigma Xi, the Optical Society of America, the Materials Research Society, and is a Fellow of the American Physical Society.

J. Gary Eden (S'75–M'76–SM'82–F'88) received the B.S. degree in electrical engineering from the University of Maryland, College Park, and the M.S. and Ph.D. degrees from the University of Illinois in 1973 and 1976, respectively. He was awarded a National Research Council Postdoctoral Research Associateship from the Naval Research Laboratory (NRL), Washington, DC, in 1975.

In November 1976 he joined the staff of the Laser Physics Branch of the NRL. During his tenure there he made several contributions to the areas of visible and ultraviolet lasers and gas laser spectroscopy. Since joining the faculty of the University of Illinois in 1979, he has conducted experiments focusing on electronic transition gas lasers and their applications. His research group has demonstrated several new molecular lasers and amplifiers in the visible and near IR (including CdBr and ZnI) and has developed laser spectroscopic techniques for studying the Rydberg states of diatomic and triatomic excimer molecules. Recently, his efforts have concentrated on laser photochemical processes for growing semiconductor and metal films and on nonlinear techniques for generating coherent VUV radiation. He has published extensively, and has been granted 11 patents.

Dr. Eden is a Fellow of the Optical Society of America and is an Associate Editor of IEEE PHOTONICS TECHNOLOGY LETTERS. He received a Research Publication Award in 1979 for his work at the NRL, in which he codiscovered the first ion-beam-pumped laser.